การรวมของอนุภาคทองคำระดับนาโนเมตรและไลโครีนเพื่อเพิ่มฤทธิ์ต้านการอักเสบ

นายวรายุกฤช พยุยงค์

วิทยานิพนธ์นี้เป็นส่วนหนึ่งของการศึกษาตามหลักสูตรปริญญาวิทยาศาสตรมหาบัณฑิต
สาขาวิชาเทคโนโลยีชีวภาพ
คณะวิทยาศาสตร์ จุฬาลงกรณ์มหาวิทยาลัย
ปีการศึกษา 2559

COMBINATION OF GOLD NANOPARTICLES AND LYCORINE FOR ENHANCING ANTI-INFLAMMATORY ACTIVITY

Mr. Varayukrit Payuyong

A Thesis Submitted in Partial Fulfillment of the Requirements

for the Degree of Master of Science Program in Biotechnology

Faculty of Science

Chulalongkorn University

Academic Year 2016

Thesis Title	COMBINATION OF GOLD NANOPARTICLES AND LYCORINE FOR ENHANCING ANTI-INFLAMMATORY ACTIVITY
By	Mr. Varayukrit Payuyong
Field of Study	Biotechnology
Thesis Advisor	Associate Professor Nattaya Ngamrojanavanich, Ph.D.
Thesis Co-Advisor	Associate Professor Nongnuj Muangsin, Ph.D.

Accepted by the Faculty of Science, Chulalongkorn University in Partial Fulfillment of the Requirements for the Master's Degree

Dean of the Faculty of Science

(Associate Professor Polkit Sangvanich, Ph.D.)

THESIS COMMITTEE

Chairman

(Associate Professor Vudhichai Parasuk, Ph.D.)

Thesis Advisor

(Associate Professor Nattaya Ngamrojanavanich, Ph.D.)

Thesis Co-Advisor

(Associate Professor Nongnuj Muangsin, Ph.D.)

Examiner

(Associate Professor Chanpen Chanchao, Ph.D.)

Examiner

(Associate Professor Aphichart Karnchanatat, Ph.D.)

External Examiner

(Prapas Khorphueng, Ph.D.)

วรายุกฤช พยุยงค์ : การรวมของอนุภาคทองคำระดับนาโนเมตรและไลโครีนเพื่อเพิ่มฤทธิ์ต้านการอักเสบ (COMBINATION OF GOLD NANOPARTICLES AND LYCORINE FOR ENHANCING ANTI-INFLAMMATORY ACTIVITY) อ.ที่ปรึกษาวิทยานิพนธ์หลัก: รศ. ดร. นาตยา งามโรจนวณิชย์, อ.ที่ปรึกษาวิทยานิพนธ์ร่วม: รศ. ดร. นงนุช เหมืองสิน, 70 หน้า.

การอักเสบเป็นการตอบสนองทางชีวภาพที่ซับซ้อนของเนื้อเยื่อที่ทำให้เกิดการอักเสบจากสิ่งแปลกปลอมเช่น เชื้อโรค สารเคมี ต้องรักษาด้วยยากลุ่มที่ไม่ใช่สเตียรอยด์ (NSAIDs) ซึ่งมีผลข้างเคียงต่อผู้ป่วย เหตุผลนี้จึงได้สนใจสารที่เกิดขึ้นตามธรรมชาติจากพืชมาพัฒนาเป็นยาเพื่อรักษาการอักเสบ ซึ่งไลโครีน (Lycorine) เป็นสารอัลคาลอยด์จากพืชวงศ์ *Amaryllidaceae* มีคุณสมบัติต้านการอักเสบ ด้วยเหตุผลเหล่านี้ไลโครีนจึงเป็นตัวเลือกในการรักษาของการอักเสบที่เกิดขึ้นได้อีกตัวเลือกหนึ่ง

อีกทั้งมีการประยุกต์ใช้อนุภาคทองคำระดับนาโนเมตร (AuNPs) ในด้านยา เนื่องจากคุณสมบัติที่มีความเสถียรทางเคมีสูง สามารถเข้ากันได้ดีกับร่างกายมนุษย์ เป็นต้น มีงานวิจัยก่อนหน้านี้ได้นำอนุภาคทองคำระดับนาโนเมตรเป็นตัวพาในระบบการนำส่งยา ใช้ในทางพันธุกรรม และโปรตีน เพื่อเพิ่มประสิทธิภาพมากขึ้น อีกทั้งยังสามารถยับยั้งการแสดงออกของ NF-kB ซึ่งเป็นโปรตีนที่ทำให้เกิดการอักเสบ ดังนั้นสารรวมระหว่างอนุภาคทองคำระดับนาโนเมตรกับไลโครีนจึงเป็นวิธีการที่น่าสนใจสำหรับรักษาการอักเสบ

ในงานวิจัยครั้งนี้ได้มีความสนใจฤทธิ์ต้านการอักเสบของสารรวมระหว่างอนุภาคทองคำระดับนาโนเมตรและไลโครีนในต้านการอักเสบที่เหนี่ยวนำจากไลโพโพลิแซ็คคาไรด์ (LPS) เหนี่ยวนำให้เกิดไนตริกออกไซด์ (NO) พบว่า ไลโครีนสามารถยับยั้งการเกิดไนตริกออกไซด์ได้ดีพอกับบูดิโซไนด์ (budesonide) ซึ่งเป็นยาแก้อักเสบที่ความเข้มข้น 10 ไมโครโมลาร์ และสารรวมระหว่างอนุภาคทองคำระดับนาโนเมตรกับไลโครีนสามารถยับยั้งการผลิตไนตริกออกไซด์ได้ที่ความเข้มข้น 10 ไมโครโมลาร์ ในงานวิจัยครั้งนี้สามารถใช้สารรวมสารรวมระหว่างอนุภาคทองคำระดับนาโนเมตรและไลโครีนในการต้านการอักเสบได้ดี จากการสังเคราะห์อนุภาคทองคำระดับนาโนเมตรด้วยพูลลูแลนพบว่าอนุภาคทองคำระดับนาโนเมตรมีขนาด 10 นาโนเมตรและรูปร่างทรงกลมจากการพิสูจน์เอกลักษณ์โดยวิธี TEM

สาขาวิชา เทคโนโลยีชีวภาพ	ลายมือชื่อนิสิต	_____
ปีการศึกษา 2559	ลายมือชื่อ อ.ที่ปรึกษาหลัก	_____
	ลายมือชื่อ อ.ที่ปรึกษาร่วม	_____

5572247423 : MAJOR BIOTECHNOLOGY

KEYWORDS: GOLD NANOPARTICLES, LYCORINE, ANTI-INFLAMMATORY ACTIVITY

VARAYUKRIT PAYUYONG: COMBINATION OF GOLD NANOPARTICLES AND LYCORINE FOR ENHANCING ANTI-INFLAMMATORY ACTIVITY. ADVISOR: ASSOC. PROF. NATTAYA NGAMROJANAVANICH, Ph.D., CO-ADVISOR: ASSOC. PROF. NONGNUJ MUANGSIN, Ph.D., 70 pp.

Inflammation is a complex biological response of tissues to harmful stimuli, such as pathogens. NSAIDs are commonly used to reduce inflammatory activities; however, some types of NSAIDs have side-effects on patients. Importantly, in this study attention the naturally occurring substances from plant to development of new drugs to treat inflammatory activities. Recently, Lycorine is one of the major alkaloids that have been isolated from the *Amaryllidaceae* plant has been reportedly possessed the anti-inflammatory activity. It is a good therapeutic candidate against inflammation which can inhibit the expression of cytokines.

Recently, gold nanoparticles (AuNPs) have been used in medicinal applications due to their unique properties such as high chemical stability, high biocompatility. AuNPs as carriers for the delivery of drugs, genetic materials and proteins resulting in enhanced their activities. For the anti-inflammation, AuNPs also inhibit the expression of NF-kappa B, a protein that acts to stimulate inflammation. In order to enhance the activation of the Lycorine, AuNPs have been employed.

Finally, this work compared the performance of lycorine, Au@P, and Ly+Au@P towards RAW 264.7 cells using LPS-induced NO tests. The results demonstrated that Lycorine could inhibit similar to budesonide in NO production. The inhibition doses was 10 µM for Ly+Au@P This work showed a successful inhibition agent derived from the excellent combination of Lycorine and Au@P. The synthesis of AuNPs using pullulan that has a particles size about 10 nm. The shape is spherical shape by TEM technigue

Field of Study: Biotechnology	Student's Signature ....
Academic Year: 2016	Advisor's Signature ....
	Co-Advisor's Signature ....

ACKNOWLEDGEMENTS

CONTENTS

LIST OF ABBBREVIATIONS

°C	degree Celsius
D_2O	Deuterium oxide
DCC	N, N'-Dicyclohexylcarbodiimide
DMAP	4-(Dimethylamino) pyridine
DMEM	Dulbecco's modified Eagle's medium (DMEM)
MTT	3-(4, 5-dimethylthiazol-2-yl)-2,5-diphenyltetrazolium bromide
DMSO	Dimethyl sulfoxide
FA	Folic acid
IR	Fourier-Transform Infrared Spectroscopy
h	hour
AuNPs	Gold nanoparticles
g	gram
LPS	lipopolysaccharide
L	liter
mg	milligram
ppm	milligram per liter
μL	microliter
μM	micro molar
mL	milliliter
min	minute
nm	nanometer
NO	Nitric oxide
NSAIDs	Non-steroidal anti-inflammatory drug
NMR	Nuclear Magnetic Resonance
P	Pullulan

LIST OF FIGURES

LIST OF TABLES

CHAPTER I
INTRODUCTION

1.1 Introduction

Nowaday, the inflammation can occur both inside and outside the body. This is caused by many factors including irritation, chemical burns and physical injury, which cause diseases such as arthritis, rheumatoid grand. These diseases require some treatment with antibiotics, the types of steroids. However, there are many side effects for patients [1]. The antibiotics in the group of non-steroidal anti-inflammatory drug (NSIADs). The group was used instead of antibiotics while there are side effects to the stomach. Then we interested to import natural substances used instead of these chemical antibiotics.

The folk medicinal plants in the family *Amaryllidaceae* that has produced a substance which has anti-inflammatory and lycorine which a substance in the group of alkaloids found in Crinum lily [2]. In the past, the Crinum lily using was heated then leaning on the stomach after giving birth to reduce inflammation from injury.

In present day, there are widely study on the biological properties of gold nanoparticles (AuNPs) using as a carrier with drug delivery system and biomolecules. The AuNPs are low toxicity (not a carcinogen) and it was used on drug delivery at concentration higher than the normal drug delivery. An anti-inflammatory effect The report has found that AuNPs spheres 21 nanometers can inhibit the expression of tumor necrosis factor alpha (TNF-α) which are stimulated inflammation in fat tissue of mice [3]. It also has the effect of inhibiting nuclear factor kappa B (NF- кB), that provokes into inflammation [4] and there are used dexamethasone as antibiotics with AuNPs can reduce the inflammation of the transplant tissue as well [5].

In addition, polysaccharide compounds such as pullulan was interested qualify as a reducing agents and a stablizing agent for the synthesis of metal particles. Pullulan is a compound of polysaccharide containing maltotriose units connected by α-1,4 and α-1,6 glycosidic bonds. It also has three unit of glucose called maltotriose by α-1,4 glycosidic bonds. Pullulan has a high water solubility and non-toxicity to the human cells. In the drug industries, pullulan was used in a drug delivery system which non-toxicity, not effects on the immune system and not a carcinogen. It also has medical applications such as wound healing.

In this research is very interesting to study the effects of combination of AuNPs and lycorine for enhancing the anti-inflammatory activity.

1.2 The objective of this research

The purpose of this study was to investigate the effect of combination of AuNPs and lycorine for enhancing the anti-inflammatory activity.

1.3 The scope of this research

The scope of this research was carried out by stepwise methods as follow:

1.3.1 Review literatures for related researcher.

1.3.2 Part I: Find the optimal conditions for the synthesis of AuNPs with pullulan

a. Characterization of the physical and chemical properties using by ^{1}H-NMR

b. Characterization of the physical and chemical properties using by FTIR

1.3.3 Part II: Find the optimal conditions for AuNPs, lycorine and combination of AuNPS and lycorine on biological assay.

a. Determination of the anti-inflammatory activity using by NO assay.

b. Determination of the cytotoxicity using by MTT technique.

1.3.4 Report, discussion and writing up thesis

CHAPTER II

THEORETICAL AND LITERATURE REVIEWS

2.1 Inflammation

Inflammation is a response of the tissues to toxic substances or destroying tissue. It is observed from the five physical symptoms of inflammation together including symptoms of inflammation are swelling, redness, heat, pain and loss of function of tissue. The inflammation is responsed by mediators such as leukotrienes, bradykinin, interleukins and substance with oxygen molecules (Reactive Oxygen Species; ROS) produced by white blood cells (neutrophils) [6]. These molecules play the important role in the destruction of pathogens, the cause of inflammation, protecting tissue from physical injury and preventing the spread of injury. Inflammation is divided into two types: The acute and chronic inflammation [2].

The acute inflammation response to intermediates instantly. It will stimulate some substance to prevent occurring harmful, the expansion of the blood vessels, increasing the flow of blood in the injured tissue which related to increasing of white blood cells, increasing the expression of adhesion molecules on endothelial cells. Followed by adhesion of leukocytes and increased vascular permeability edema and leukocyte infiltration into the tissue [7]. After that, the white blood cells swallowed bacteria or antigen. The ROS and proteases enzyme were released. These may cause more damaged tissue [8]. The effect of these process in the production of chemical mediators of inflammation and lead to more inflammation, too. This cytokine is response for regulation of white blood cells (such as IFN-α) or inhibited the response of the immune system (such as IL-10). For examples, the acute inflammation including the severe shock and the inflammation of pancreas [7, 9] by the production of inflammatory mediators (IL-10 and lipoxins) [6, 8], which have protected the inflammation. The inflammation is eliminated by white blood cells that will move to the area of injury and apoptosis.

The chronic inflammation can occur for a long time. The changing nature of the inflammatory cell types by region. Examples of diseases caused by chronic inflammation including rheumatoid arthritis, asthma and inflammatory bowel disease and many other diseases associated with inflammation (atherosclerosis, autoimmune diseases, Alzheimer's disease, cancer, trauma, ischemia, diabetes, etc.) [10, 11], which need to treated with antibiotics in the steroids group. However, there are side effects to the patient. Futhermore, the antibiotics in NSIADs group is commonly used to cure

the disease but there are side effects to the stomach. Natural products were interested in the study of biological activities. In this work, the researcher interested in the folk medicinal plant, that is lycorine.
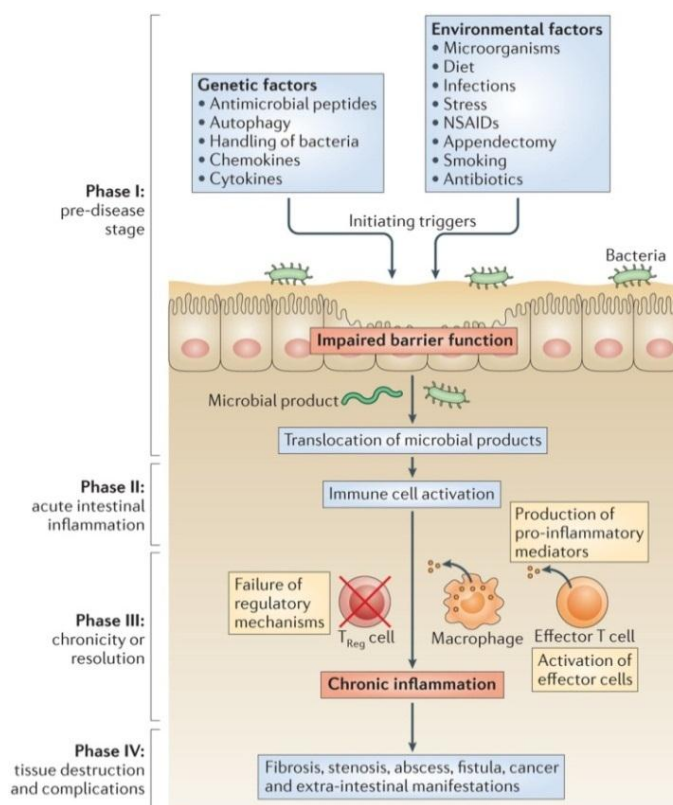
Figure 2.1: Example of chronic inflammation; Conceptual framework for the pathogenesis of Inflammatory bowel disease (IBD). Genetic and environmental factors induce impaired barrier function in the intestinal mucosa. Initiating triggers may involve infections in some patients. Altered barrier function subsequently induces the translocation of commensal bacteria and microbial products from the gut lumen into the bowel wall, which leads to immune cell activation and cytokine production. If acute mucosal inflammation cannot be resolved by anti-inflammatory mechanisms and the suppression of pro-inflammatory immune responses, chronic intestinal inflammation develops. In turn, chronic inflammation may cause complications of the disease and also tissue destruction, which are both driven by mucosal cytokine responses. DC, dendritic cell; IBD, inflammatory bowel disease; NSAIDs, non-steroidal anti-inflammatory drugs; T_{Reg} cell, regulatory T cell [12].

2.2 Extracted lycorine from *Crinum asiaticum* Linn. (Crinum lily)

The natural products were interested in the study of biological activities like Inhibited cancer, the anti-inflammatory activity. The natural substance is toxic less than chemical products. In this work, the researcher interested in a natural compound of the folk medicinal plant, that is lycorine.

Lycorine is a major alkaloid found in the leaf and root bulb of the amaryllidaceae family plants. This alkaloid has been shown to behave as potent therapeutic agent in numerous experimental models. It possesses many pharmacological activities such as hepatoprotective, antioxidant, anti-inflammatory, antibacterial activities and analgesics agents [13]. In previous study, the researchers have been combined the natural product (lycorine) with gold nanoparticles (AuNPs) for enhancing the activities.
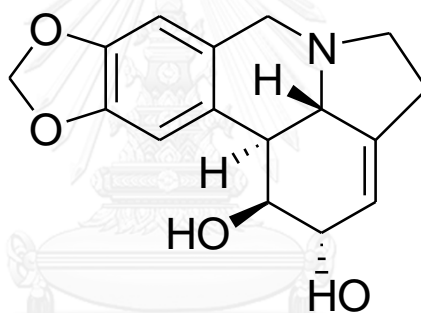
Figure 2.2: Chemical structure: lycorine [14].

The present studies, lycorine was to investigate the anti-inflammatory activity;

In 1999, Mikami *et al.* [15] and in 2008 Kim *et a.l* [16] presented the anti-inflamtory effect of lycorine which is major components in Crinum lily (*C. asiaticum* var. siacum) It can inhibit the Calprotetin-inflammatory cells, which is found in the cytosol of neutrophils, and also the cause of inflammation.

In 2011, Saltan *et al.* [17] studied the anti-inflamtory effect of lycorine from *Sternbergia fisheriana* (Herbert) Rupr. at concentration 1.0 และ 1.5 mg/kg can inhibit the inflammation at 53.45 and 36.42%, respectively.

In 2011 Kang *et al.* [18] reported the effects of inhibition of lipopolysaccharide (LPS) in RAW 264.7 cells with lycorine. It inhibited LPS which is a major component of the cell wall of gram-negative bacteria. It can reduce the

release of NO, PGE2, TNF-**α**, and IL-6, which is a group of inflammatory substances in RAW 264.7 cell lines as well.

2.3 Anti-inflammatory effects

2.3.1 Non-steroidal anti-inflammatory drugs (NSAIDs)

The Non-steroidal anti-inflammatory drugs (NSAIDs) are widely used for both chronic and acute musculoskeletal and inflammatory conditions. Most of NSAIDs made up of analgesics [19].

2.3.2 Lipopolysaccharides

Lipopolysaccharide (LPS) are generally considered toxic components of the gram-negative bacterial outer membrane with potent immunomodulating and immunostimulating properties [20]. LPS is a potent macrophage-activating stimulus which induces expression of many genes necessary for the execution of host defense function [21]. This antigen can activate macrophages to release some inflammatory mediators such as NO, TNF-α and PGE_2 [22].

2.4 Anti-inflammatory drug

2.4.1 Budesonide

Glucocorticoids inhibit practically all steps in the inflammatory response including cytokine production and adhesion molecule up-regulation on a variety of cell types. For instance, budesonide is an anti-inflammatory corticosteroid, which have been shown to inhibit ICAM-1 and VCAM-1 expression on activated epithelial and endothelial cells78 and on fibroblasts. Glucocorticoids also inhibit GM-CSF, IL-8 and IL-6 production by epithelial cells and fibroblasts [23]. In addition, airway inflammation is an important element in the pathophysiology of stable asthma and is heightened during asthma exacerbations. For anti-inflammatory agents, notably glucocorticosteroids, are therefore commonly used for the treatment of moderate and severe asthma. Inhaled glucocorticosteroids (ICS) have been recommended [24]. Budesonide has been used a number of autoimmune and autoinflammatory deseases. Dosed budesonide is effective therapy for asthma and is believed to act by reducing and preventing respiratory tract inflammation [25].
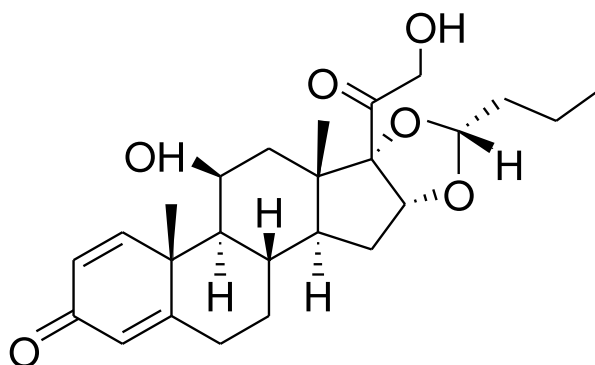
Figure 2.3: Chemical structure: budesonide [25].

2.5 Cancer

Cancer is a leading cause of death worldwide and account for 7.6 million deaths (around 13% of all deaths) in 2008. Cancer is a large group of diseases that can affect any part of the body. Other terms used are malignant tumors and neoplasms. One defining feature of cancer is the rapid creation of abnormal cells that grow beyond their usual boundaries, and which can then invade adjoining parts of the body and spread to other organs. This process is referred to as metastasis. Metastases are the major cause of death from cancer [26].

2.6 Anti-cancer drugs

The anticancer drug, also called antineoplastic drug, is effective in the treatment of malignant or cancerous disease. There are several major classes of anticancer drugs: these include alkylating agents, antimetabolites, natural products, and hormones [27].

2.6.1 Doxorubicin

Doxorubicin (Dox) is a well-known semisynthetic, anthracycline antibiotic partly obtained from bacterial species and widely used in cancer therapeutics including hematological malignancies (blood cancers, like leukaemia and lymphoma), many types of carcinoma (solid tumors) and soft tissue sarcomas. Dox sold under the trade names Adriamycin. It is often used in combination chemotherapy as a component of various chemotherapy regimens [28].
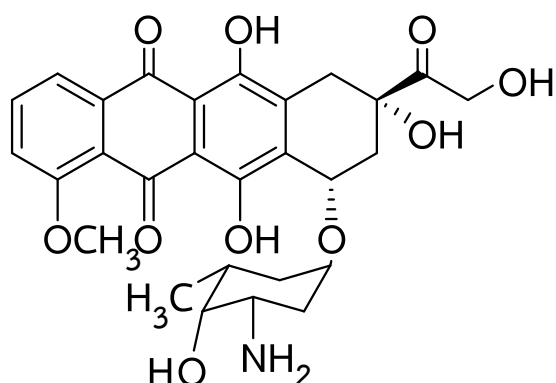
Figure 2.4: Chemical structure: Doxorubicin [29].

2.7 Polymer

The polysaccharide compounds, was interested properties as a reducing agent and a stablizing agent for the synthesis of metal particles. Pullulan is containing maltotriose units connected by α-1,4 and α-1,6 glycosidic bonds (Figure 2.5). There are three units of glucose called maltotriose. Pullulan also has a high water solubility and non-toxicity to the human cells which was used in a drug delivery system which non-toxicity, not effects on the immune system and not a carcinogen in drug industry. In addition, pullulan has medical applications such as wound healing.

Pullulan, which is a highly water-soluble, neutral, linear polysaccharide, has properties of biocompatibility and biodegradability. These attributes have been exploited in the extensive biomedical use of pullulan as a nanomaterial [30].
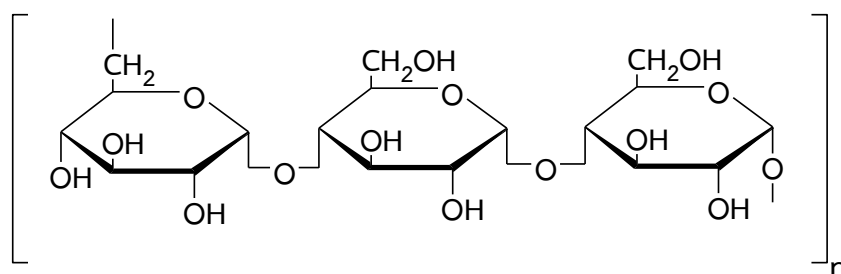
Figure 2.5: Chemical structure: pullulan [31].

2.8 Gold nanoparticles (AuNPs)

In the recent studies on inflammation and inflammation of natural substances has begun to study metal nanoparticles such as gold nanoparticles (AuNPs). Gold nanoparticles (AuNPs) provide non-toxic carriers for drug and gene delivery applications [32]. The studies found that has low toxicity property and not a carcinogen. It also has anti-inflammatory activity as well.

In 2002, Hickey *et al.* [5] studied antibiotics, dexamethasone with AuNPs can reduce tissue inflammation from organ medical implantation.

In 2011, Franca *et al.* [33] reported that the amount of AuNPs were low toixicity (0.005 EU / ml) and found that the particles do not cause the release of cytokines in white blood cells as well.

In 2013, Chen *et al.* [3] performed that the size of AuNPs are 21 nanometers, can inhibit the expression of TNF-**α** in fat tissue of mice after intraperitoneal injection. It is shown that, AuNPs has the anti-inflammatory activity.

And in 2013, Sumbayev *et al.* [34] explained AuNPs was directly connected with IL-1**β** inhibitors can cause inflammation.

2.9 Folic acid

Folic acid has emerged as an optimal targeting ligand for selective delivery of attached imaging and therapeutic agents to cancer tissues and sites of inflammation. its ease of conjugation to both therapeutic and diagnostic agents. Cancers found to overexpress FR include cancers of the ovary, lung, breast, kidney, brain, endometrium, colon, and hematopoietic cells of myelogenous origin. Because activated macrophages are implicated in such pathologies as rheumatoid arthritis, psoriasis, Crohn's disease, systemic lupus erythematosus, atherosclerosis, diabetes, ulcerative colitis, osteoarthritis, glomerulonephritis, and sarcoidosis, applications for folate targeting now also include most inflammatory diseases. While FR-directed antifolates have proven useful in the treatment of some of the above diseases,3–7 this Account will focus on the discovery and development of folate receptor-targeted drugs for the diagnosis and therapy of these pathologies [35].
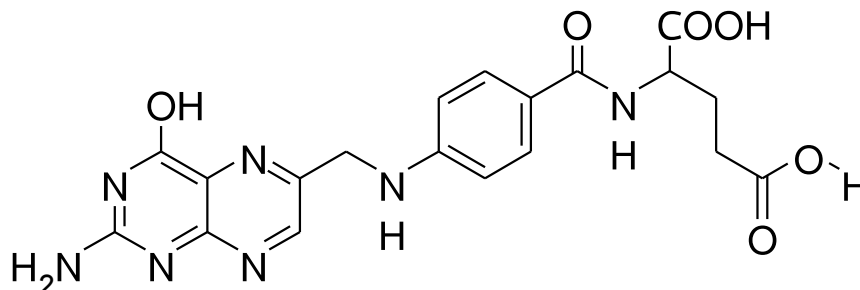
Figure 2.6: Chemcial structure: folic acid [36].

2.10 Analytical instruments

2.10.1 Ultraviolet-Visible (UV-vis) spectroscopy

UV-vis spectroscopy, the instrument employed for spectra collection was an Agilent 8453E UV–vis spectroscopy system (Agilent Technologies, Waldbronn, Germany). The spectra were collected using a UV–vis Chem Station Rev. A.06.03 (Hewlett–Packard, USA). The absorbance spectra were recorded in triplicate. The optical properties of the colloidal gold solution were monitored on a spectrophotometer in the range of 300–700 nm. The instrument was equipped with a Quartz cuvettes with 1 cm optical length. This short pathlength enabled to obtain absorbance values within the appropriate range regarding to accuracy and precision specified by the spectrophotometer characteristics manual.

2.10.2 Scanning Electron Microscopy (SEM)

A Scanning Electron Microscope (SEM) is a powerful magnification tool that utilizes focused beams of electrons to obtain information. The high-resolution, three-dimensional images produced by SEMs provide topographical, morphological and compositional information makes them invaluable in a variety of science and industry applications. The SEM can be as essential research tool in fields such as life science, biology, gemology, medical and forensic science.

2.10.3 Transmission Electron Microscopy (TEM)

A Transmission Electron Microscope (TEM) utilizes energetic electrons to provide morphologic, compositional and crystallographic information on samples. At

a maximum potential magnification of 1 nanometer, TEM are the most powerful microscopes. TEM produce high-resolution, two-dimensional images, allowing for a wide range of educational, science and industry applications. The TEM is ideal for a number of different fields such as life sciences, nanotechnology, medical, biological and material research, forensic analysis, gemology and metallurgy as well as industry and education. TEM provide topographical, morphological, compositional and crystalline information.

2.10.4 ^{1}H Nuclear Magnetic Resonance spectroscopy (^{1}H-NMR)

NMR spectroscopy is an analytical instument used in chemistry for identification and quantification of chemical compositions in a sample. NMR has become an important analytical tool that can be used to study molecular structures as well as molecular dynamics, including organic chemistry, inorganic chemistry, structural biology, biochemistry, physics, biology, polymer chemistry, drug discovery, material science, in addition to several applications in modern medicine [37].

2.10.5 Fourier-Transform Infrared Spectroscopy (FTIR)

FTIR spectroscopy is a vibrational spectroscopic technique that can be used to measure characteristics within compounds that would allow accurate and precise assignment of the functional groups, bonding types, and molecular conformations [38]. FTIR employs the different chemical functional groups absorb at specific wavenumbers in the infrared range (4000–400 cm^{-1}). Thus, the spectra analysis gives the data on functional groups and molecular structures that can be useful for the identification of specific compounds [39].

2.11 Nitric oxide (NO) determination

Nitric oxide (NO) is a free radical species that is intricately involved with the innate immune response [40]. Nitric oxide (NO) is synthesized by nitric oxide synthase (NOS) from L-arginine using NADPH and molecular oxygen in various animal cells and tissues., is a free radical and an intercellular messenger produced by a variety of mammalian cells. NO shows cytotoxicity and tissue damage, whereas nanomolar concentrations of NO produced by constitutive forms of NOS are essential to maintain normal cellular functions. NO is involved in various biological processes including inflammation and immunoregulation. Therefore, inhibition of NO production by iNOS may have potential therapeutic value when related to inflammation and septic shock [41].

Nitrite is detected and analyzed by formation of a red pink colour treatment of a NO_2^--containing sample with the Griess reagent. When sulphanilic acid is added, the nitrites form a diazonium salt. When the azo dye agent (N-alpha-naphthyl-ethylenediamine) is added a pink colour develops. This diamine is used in place of the simpler and cheaper alpha-naphthylamine because this latter is a potent carcinogen and moreover the diamine forms a more polar and hence a much more soluble dye in acidic aqueous medium [42].

NO production by measuring its production against LPS-stimulated RAW 264.7 cells. The pink solution is measured by UV-visible spectrophotometer. The absorbance was measured at 540 nm on ELISA reader. The NO inhibitory activity can be calculated the concentration of nitrite by comparison to calibration curve of sodium nitrite standard.
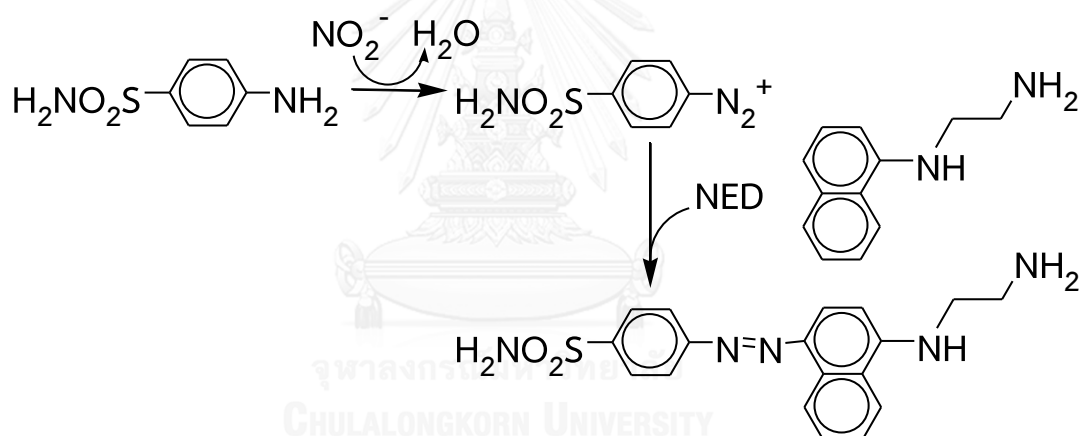
Figure 2.7: Chemical reactions involved in the measurement of NO_2^- using the griess reagent system [43].

2.12 MTT assay

MTT assay is a colorimetric assay for evaluating cell metabolic activity. NAD(P)H-dependent cellular oxidoreductase enzymes may indicate the number of viable cells. These enzymes are ability of reducing the yellow [3-(4,5-dimethylthiazol-2-yl)-2,5-diphenyltetrazolium bromide, MTT] tetrazole dye to its insoluble [(*E,Z*)-5-(4,5-dimethylthiazol-2-yl)-1,3-diphenylformazan, formazan], which has a purple color in living cells. A solubilization solution (usually dimethyl sulfoxide, DMSO) is added to dissolve the insoluble purple formazan production into a colored solution.

The absorbance of this colored solution can be quantified by measuring at a certain wavelength (usually 540 nm) by a spectrophotometer. The degree of light absorption depends on the solvent.
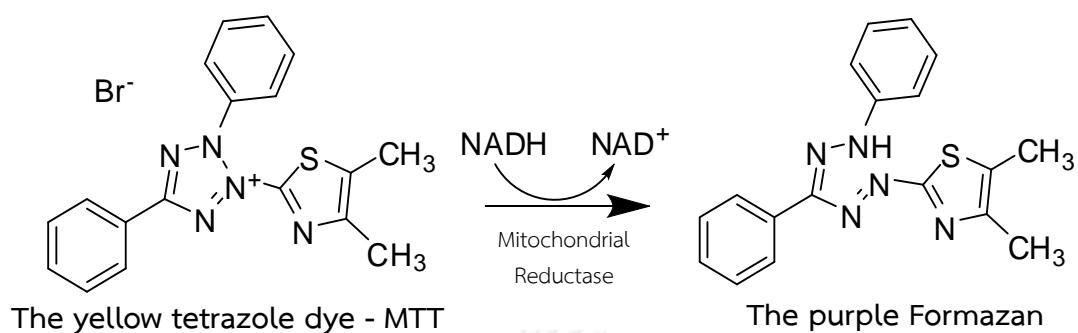
Figure 2.8: Mitochondrial reduction of MTT to blue formazan product [44].
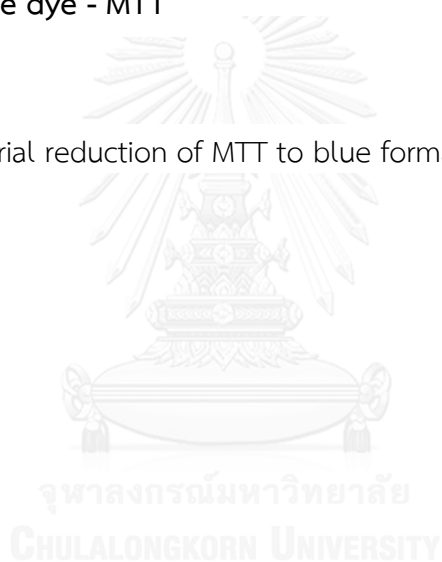
CHAPTER III
EXPERIMENTAL

3.1 MATERIALS AND INSTRUMENTS

3.1.1 Equipments

- Autopipette: Thermo Fisher Scientific Inc., USA

- Beaker: Isolab, Germany

- Dialysis bag: Membrane Filtration Products, USA

- Hot air oven: Memmert, Germany

- Hot plate: Becthai Bangkok Equipment & Chemical, Thailand

- Fourier-transform Infrared Spectroscopy (FTIR): Thermo, Finland

- Laboratory fume hood: Asian chemicals & engineering, Thailand

- Magnetic stirrer: Brand, Germany

- Nuclear Magnetic Resonance (NMR): Bruker, Belgium

- NMR tube: Schott duran, Denmark

- Pipette: Witeg, Germany

- Scanning Electron Microscopy (SEM): Jeol, USA

- Thermometer: Brannan, England

- Transmission Electron Microscopy (TEM): Jeol, USA

- Universal indicator: Merck, Germany

- UV-Visible Spectrophotometer: Agilent Technologies Training Center Bangkok, Thailand

- Vortex: Schott, Germany

3.1.2 Chemical and solvents

- Deuterium oxide (D_2O): Merck, Germany

- N,N'-Dicyclohexylcarbodiimide (DCC): Sigma-Aldrich Chemistry Inc., USA

- 4-(Dimethylamino) pyridine (DMAP): Sigma-Aldrich Chemistry Inc., USA

- Dimethyl sulfoxide (DMSO): Merck, Germany

- Folic acid ($C_{19}H_{19}N_7O_6$): Sigma-Aldrich Chemistry Inc., USA

- Potassium chloride (KCl): Merck, Germany

- Potassium dihydogen phosphate (KH_2PO_4): Merck, Germany

- Pullulan [$(CH_2O)_n$]: Tokyo Chemical Industry Co., Ltd., Japan

- Sodium chloride (NaCl): Merck, Germany

- di-Sodium hydrogen phosphate (Na_2HPO_4): Merck, Germany

3.1.3 Cell culture and Materials
3.1.3.1 Cell lines

- Murine Macrophage Leukemia cancer cell (RAW 264.7): Cells line Service, Germany

3.1.3.2 Media and Enzyme

- Fetal Calf Serum (FCS): Sigma-Aldrich Chemistry Inc., USA

- Trypsin: Thermo Fisher Scientific Inc., USA

- Dulbecco's modified medium (DMEM): Sigma-Aldrich Chemistry Inc., USA

3.1.3.3 Cell culture apparatus

- Centrifuge: Thermo Fisher Scientific Inc., USA

- Counting slide: Boeco, Germany

- Dropper: Isolab, Germany

- Forceps: Thermo Fisher Scientific Inc., USA

- Incubator: Thermo Fisher Scientific Inc., USA

- Lamina air flow hood: Cambridge, USA

- Microscope: Nikon, Japan

- Micropipette: Thermo Fisher Scientific Inc., USA

- Multichannel pipette: Thermo Fisher Scientific Inc., USA

- Rubber bulb: Isolab, Germany

- Tube: Eppendorf, Malaysia

- Vortex: Schott, Germany

- 96-well plates: Corning Incorporated, USA

3.1.4 MTT assay materials and Apparatus

- 3-(4,5-dimethylthiazol-2-yl)-2,5-diphenyltetrazolium bromide (MTT): Thermo Fisher Scientific Inc., USA

- Dimethyl sulfoxide (DMSO): Merck, Germany

- Microplate reader spectrophotometer: Thermo Fisher Scientific Inc., USA

- Normal saline solution (NSS): Sigma-Aldrich Chemistry, USA

3.1.5 Reagent for anti-inflammatory assay

- Griess reagent (modified): Sigma-Aldrich Chemistry, USA

- Lipopolysaccharide (LPS): Sigma-Aldrich Chemistry, USA

3.2 Materials

3.2.1 Lycorine

Lycorine was used in this study purchased from Xi'an Natural Field Bio-Technique Co., Ltd., China.

3.3 Synthesis of folic acid conjugated pullulan

The synthesis of folic acid conjugated pullulan (P-FA) was carried out according to Lee *et al*. [45]. Briefly, the pullulan (1000 mg) was dissolved in DMSO

(25 mL) for 30 min with DMAP (20 mg). Folic acid (200 mg) was dissolved in DMSO (10 ml) and DCC (60 mg) for 30 min. Folic acid and DCC solution were added into the pullulan solution and stirred for 48 h at room temperature. The resulting solution was filtered to remove by products and dialyzed against deionized water for 3 days. The analyzed solution was further precipitated in acetone and dried in a oven for 2 days. The synthesized P-FA was analyzed with ^{1}H-NMR and FTIR.

3.4 Synthesis of Gold nanoparticles using with pullulan/pullulan-folic acid

The initial synthesis of AuNPs was carried out in a mixture containing various volumes of pullulan, 0.1 mL of 0.1 M NaOH and the volume was made up to 2 mL by adding the appropriate amount of deionized water. The tube was placed at magnetic stirrer and stirred to ensure the completed mixing at 80±1℃ for 15 min. After that, different volumes (0-160 μL) of 10^3 ppm $HAuCl_4$ were added into the mixture for 60 min. The color change was occurred from colorless to red colored suspension that confirmed the formation of Au@P. The absorbance was measured at wavelength range of 400-700 nm on UV-visible spectrophotometer.

In addition, Synthesis of AuNPs using with P-FA was carried out in a mixture containing 2% of pullulan-FA, 100 μM NaOH and distilled water in the same condition of AuNPs stabilized pullulan. The color change was occurred from colorless to green colored suspension that confirmed the formation of Au@P-FA. The absorbance was measured at wavelength range of 400-700 nm on UV-visible spectrophotometer.

3.5 Analytical instruments

3.5.1 Ultraviolet-Visible (UV-vis) spectroscopy

UV-vis spectroscopy, the instrument employed for spectra collection was an Agilent 8453E UV–vis spectroscopy system (Agilent Technologies, Waldbronn, Germany). The spectra were collected using a UV–vis Chem Station Rev. A.06.03 (Hewlett–Packard, USA). The absorbance spectra were recorded in triplicate. The working range was 300– 700 nm. The instrument was equipped with a quartz cell with a pathlength of 0.1 cm. This short pathlength enabled to obtain absorbance values within the appropriate range regarding to accuracy and precision specified by the spectrophotometer characteristics manual.

3.5.2 Scanning Electron Microscopy (SEM)

SEM samples were mounted onto an aluminum stub using double-sided carbon adhesive tape and coated with gold-palladium. Scanning was performed under high vacuum and at ambient temperature using a beam voltage of 15 KeV.

3.5.3 Transmission Electron Microscopy (TEM)

TEM samples were prepared by dropping an aqueous solution onto copper grids. The micrographs were obtained on a transmission electron microscope (JEM-2100) operated at 120 KeV and equipped with an enery-dispersive X-ray spectrometer.

3.5.4 ^{1}H-Nuclear Magnetic Resonance (^{1}H-NMR)

The ^{1}H-NMR spectra at 400 MHz was measured on a Varian Mercury plus spectrometer. All chemical shifts (δ) values were reported in part per million (ppm) relative to the residual proton in deuterated solvents peak using D_2O and DMSO-d_6 solvents as internal references. Coupling constants (J) were reported in Hertz (Hz). The ^{1}H-NMR data were processed with the MestReNova software. Briefly, D_2O solvent was used to dissolve pullulan and the synthesized P-FA while DMSO-d_6 solvent was used to dissolve folic acid. ^{1}H NMR was measured the degree of substitution (DS) of Folic acid in P-FA. The DS was calculated using the data obtained from the ^{1}H NMR spectra according to Eq (1);

$$\%DS = \left[\frac{(ArH)}{(H1)} \right] \times \frac{1}{5} \times 100 \tag{1}$$

Where (ArH) is the integration area of Aromatic at 8.57, 7.50 and 6.63 ppm, respectively and (H1) is the integration area of α-(1,4) and α-(1,6) linkage of pullulan at (5.22,5.18) and 4.77 ppm, respectively.

3.5.5 Fourier-Transform Infrared Spectroscopy (FTIR)

FTIR spectra of dried samples were acquired with a Nicolet 6700 FTIR spectrometer in the region over the 4000 – 400 cm^{-1} wavenumber range at a resolution of 4 cm^{-1} (32 averaged scans). FTIR is a method of measuring infrared absorption and emission spectra. The spectral features are reported in wavenumber (cm^{-1}). FTIR information was assessed with the OMNIC software.

3.5.6 Energy Dispersive X-ray Spectrometry (EDX)

The analytical technique used for the elemental analysis or chemical characterization of a   sample. It relies on an interaction of some source of X-ray excitation and a sample. Its characterization capabilities are due in large part to the fundamental principle that each element has a unique atomic structure allowing a unique set of peaks on its electromagnetic emission spectrum (which is the main principle of spectroscopy). Scanning was performed under high vacuum and at ambient temperature using a beam voltage of 20 KeV.

3.6 Biological assay

3.6.1 Anti-inflammatory activity

3.6.1.1 Cell culture

The murine macrophages RAW 264.7 cells were grown in DMEM medium supplemented with 10% (v/v) of fetal bovine serum (FCS) at 37°C, 5% CO_2 atmosphere.

3.6.1.2 Calibration curve of nitrite standard

Stock solution of 0.69 mg/mL Sodium Nitrite ($NaNO_2$) was prepared by sodium nitrite ($NaNO_2$) in deionized water (DW). Then, The concentrations of nitrite performed 10 serial dilutions (0, 0.5, 1, 2, 5, 10, 20, 40, 60 and 80 µM) in triplicate down the 96-well plate (100 µL/well). Added 100 µL of Griess reagent (Figure 2.6) and incubated at room temperature for 15 min (dark condition). Absorbance was measured at 540 nm on ELISA reader.

3.6.1.3 NO determination

Briefly, the RAW 264.7 cells were incubated in 96-well plates at a density of 1.44×10^5 cells/well (8×10^5 cells/mL) at 180 µL of Dulbecco's modified Eagle's medium (DMEM) for 24 h. After pre-incubation of RAW 264.7 cells, the DMEM medium was removed 10 µL and replaced with fresh medium containing various concentrations of each compounds (0-100 µM) and then were incubated with 2 µg/mL of LPS (500 µg/mL) for stimulated NO production for 24 h. The 100 µL of supernatant was added in new 96-wells plates and mixed with 100 µL of Griess reagent in plates. Subsequently, the mixture was incubated at room temperature for 15 min at the dark condition. The absorbance was measured at 540 nm on ELISA reader. Fresh culture medium was used as a blank in every experiment. The NO

inhibitory activity can be calculated the concentration of nitrite by comparison to calibration curve of sodium nitrite standard [46].

3.6.2 Anticancer assay

3.6.2.1 Cell culture

The murine macrophages RAW 264.7 cells were grown in DMEM medium supplemented with 10% (v/v) of fetal bovine serum (FCS). Cultured cell lines were incubated in humidified atmosphere of 5% CO_2 atmosphere at 37°C and then it was sub-cultured by trypsin enzyme every three days (72 h).

3.6.2.2 Cytotoxicity by MTT assay

The MTT colorimetric method was measured according to the procedure modified by Yang *et al.* [46]. Briefly, the murine macrophages RAW 264.7 cells were incubated in 96-well plates at a density of 5×10^3 cells/well for 24 h. Thus, 20 µL of treated medium was removed and added with various concentrations of treat compounds (0-100 µM) for 2 days. After that, the medium was incubated with 10 µL of MTT (5 mg/mL) for 4 h. at 37°C. Hence, the supernatants were removed, the dark violet crystals were dissolved in 150 µL of DMSO and absorbance was measured at 540 nm on ELISA reader. The percentage of dead cells was determined relative to the control group. The data that were collected for triplicates and calculated as;

$$\% \text{ Cell viability} = \frac{\text{Absorbance of treated cell}}{\text{Absorbance of untreated cell}} \times 100 \qquad (2)$$

$$\% \text{ Cytotoxicity} = 100 - \text{percentage of cell viability} \qquad (3)$$

3.7 Combination Index

Combination index (CI) is theory of Ting-Chao Chou who derived the principle for multiple drug effect interactions, and offers quantitative definition for additive effect (CI = 1), synergism (CI < 1), and antagonism (CI > 1) in drug combinations using computerized simulations [47]. CI information was assessed with the CompuSyn software [47].

3.8 Determination of the anti-inflammatory results

The value of OD_{540} was obtained for calculation. The medical effect, or

$$\text{Inhibition rate } (fa) = 1 - \frac{\text{Mean value of OD of all groups tested}}{\text{Mean value of OD of control samples}} \quad (4)$$

According to the median-effect equation: $fa/fu = \left(\dfrac{D}{D_m}\right)^m$ $\quad (5)$

Long was applied to both ends: $\log fa/fu = m \log D - m \log Dm$

If $a = -m \log D_m$

  $b = m$

  $x = \log D$

  $y = \log fa/fu$

by substitution with the median-effect equation: $y = bx - a$

in which fa is the medical effect, $fu = 1 - fa$

D is the drug concentration, m is the slope

D_m is the median concentration

According to the above equation, the various median-effect concentrations of the two agents when used separately and in combination, Dm ($\log Dm = -a/m$) was calculated, and the various drug concentrations needed for the two agents applied separately and jointly for different effects could be obtained, $D = Dm (fa/fu) l/m$, and finally the combination index of the two drugs when applied jointly for various effects was calculated:

$$\text{Combination Index CI} = \frac{D_1}{D_{x1}} + \frac{D_2}{D_{x2}} + \frac{D_1 D_2}{D_{x1} D_{x2}} \quad (6)$$

D_1 and D_2 are the concentrations of each drug needed for the effect of X when applied jointly, D_{x1} and D_{x2} are the concentrations of each drug needed for the effect of x when applied separately, CI<I means synergistic, CI= means additive, and CI>I means antagonistic [48].

CHAPTER IV
RESULTS AND DISCUSSION

4.1 Synthesis and characterization of Au@P

Formation of the metal nanoparticles by reduction of pullulan may be easily followed by UV visible spectroscopy. It is well known that AuNPs exhibit red colors. The color arising due to excitation of surface plasmon vibrations in the metal nanoparticles [49].

4.1.1 Ultraviolet-visible (UV-vis) spectroscopy

In the present study, we interested to use the reducing and stabilizing nature of biopolymer, pullulan for the synthesis of gold nanoparticles. The pullulan was stabilized gold nanoparticles (Au@P) allowed the attachment of a large number of small molecules which will exclusively target the cancer cells and inflammatory cells.

The initial synthesis of AuNPs was carried out in a mixture containing pullulan, NaOH and distilled water. Then, $HAuCl_4$ was added into the mixture in hot water. The color change was occurred from colorless to red colored suspension. The absorbance was measured on UV-visible spectrophotometer.

The UV-vis spectra showed the absorption peak in Figure 4.1A. We synthesized AuNPs using various volume of $HAuCl_4$ from 100 μL to 160 μL of $HAuCl_4$. The Au@P at 150 μL of $HAuCl_4$, 100 μL (0.1 M NaOH), was the optimum condition with the maximum absorption of 0.228 and the wavelength average remained at 520 nm and finally, the color of solution turned to red (Figure 4.2C).

Furthermore, The UV–Vis spectra of AuNPs reduced with different concentrations of pullulan (1-3%) were illustrated in Figure 4.1B. the volume of $HAuCl_4$ at 150 μL, 2%P was maximum absorption of 0.3513 that higher than other conditions and wavelength average is 520 nm. Furthermore, These spectra have a strong absorption feature at ～520 nm due to the characteristic surface plasmon resonance of AuNPs [50]. The condition Au@P (150 μL of $HAuCl_4$, 2% P, 100 μL of 0.1 M NaOH) was studied on cytotoxicity by MTT assay and anti-inflammatory activity.
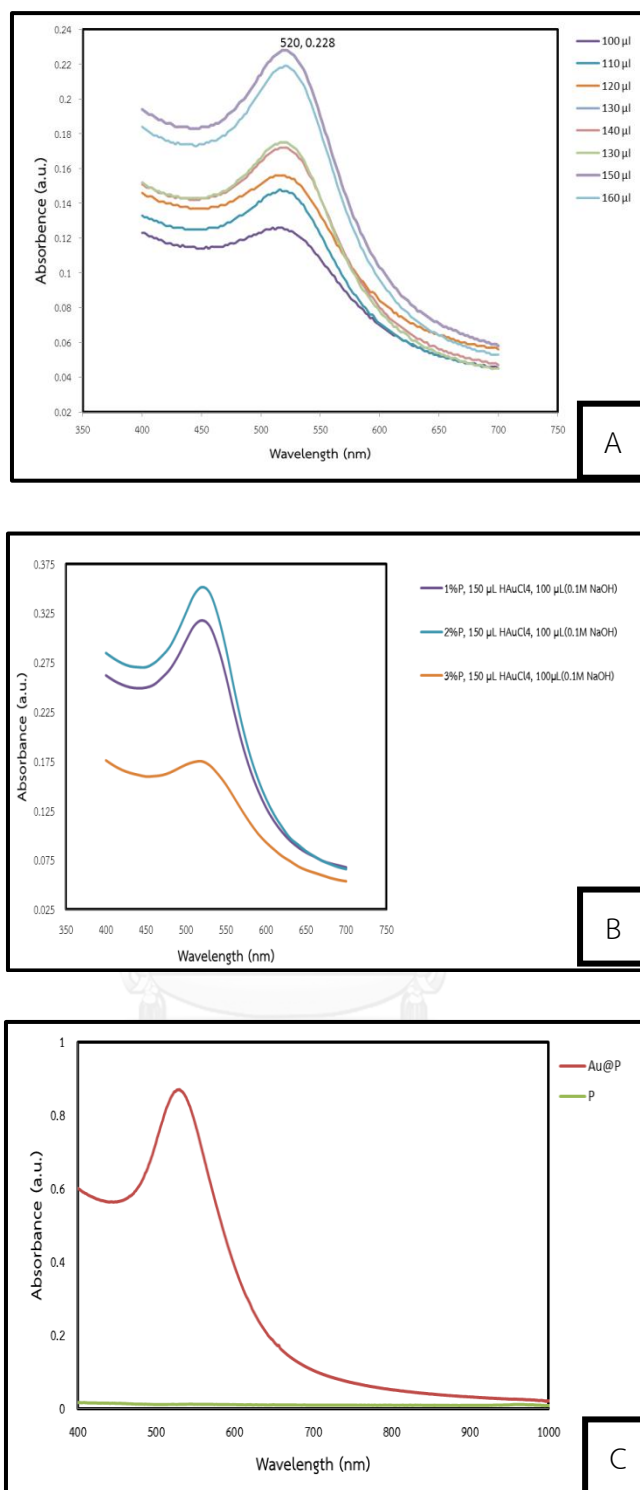
Figure 4.1: The absorption spectra of Au@P were measured at wavelength range of 400-700 nm on microtiter plate reader; (A) various volumes of HAuCl$_4$, (B) various concentrations of pullulan, 2% P, (C) 150 µL of HAuCl$_4$, 100 µL (0.1 M NaOH).
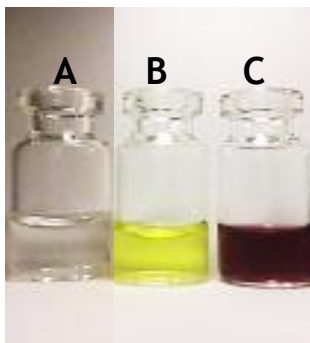
Figure 4.2: The color of mixture solution depending on our condition; (A) 2% (w/v) of P; (B) 10^3 ppm of $HAuCl_4$; (C) Au@P at 2% P, 150 μL of $HAuCl_4$, 100 μL (0.1 M NaOH).

4.1.2 Morphology of Au@P

4.1.2.1 Scanning Electron Microscopy (SEM)

The Au@P was used in pharmaceutical application, particularty as a vehicle for controlled drug delivery. In the present study, we took advantage of the reducing, stabilizing, and biocompatible properties of pullulan for the synthesis of AuNPs. The morphology of synthesized AuNPs by a range of techniques including scanning electron microscopy (SEM) and transmission electron microscopy (TEM). The SEM images of AuNPs prepared at 2% P, 150 μL of $HAuCl_4$, 100 μL (0.1 M NaOH) were shown in Figure 4.3. The morphology was clear. The shape of the particles was observed as a cubic-like structure. The particles are well dispersed with a size distribution and an average size of 1 μm. Therefore, the higher concentration of pullulan was not studied.
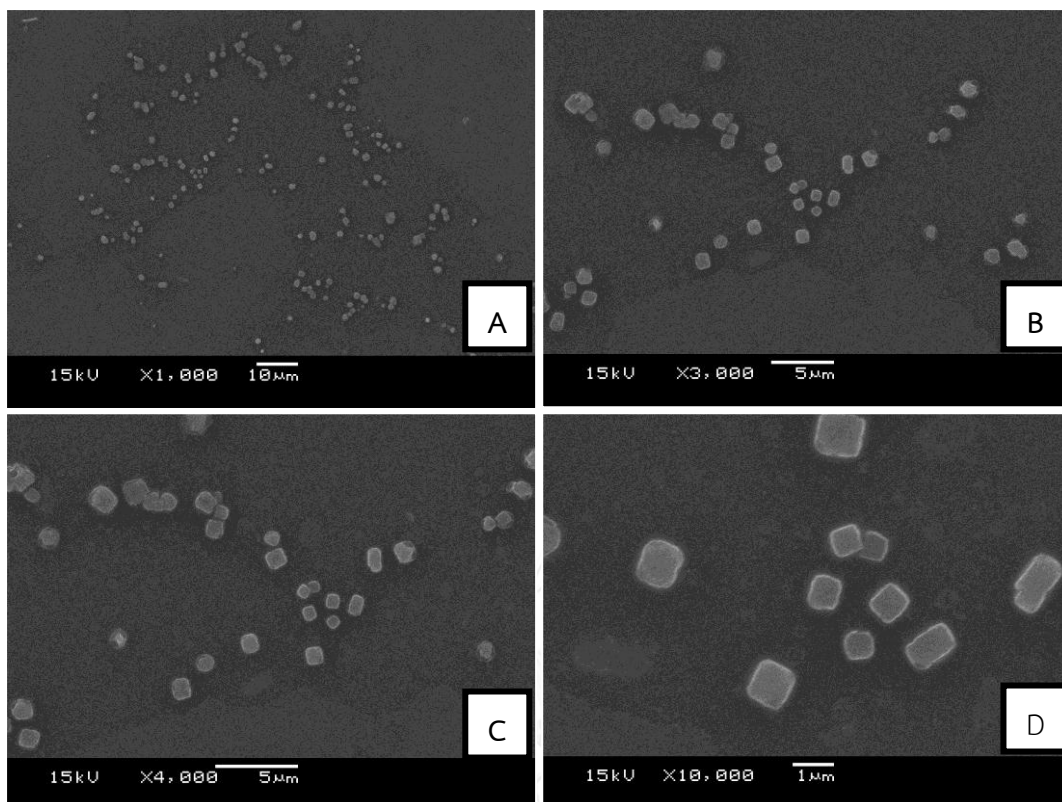
Figure 4.3: SEM images of Au@P at 2% P, 150 µL of HAuCl$_4$, 100 µL (0.1 M NaOH); (A) 1000X; (B) 3000X; (C) 4000X and (D) 10000X

4.1.2.2 Transmission Electron Microscopy (TEM)

The TEM images recorded from as-synthesized AuNPs (Figure 4.4) revealed that the nanoparticles were well dispersed with a narrow size distribution and an average size of 10 nm (Figure 4.4A-B). The morphology of Au@P was the spherical shape. In subsequent experiments, Therefore, pullulan-folic acid (Au@P-FA) stabilized gold nanoparticles was not studied.
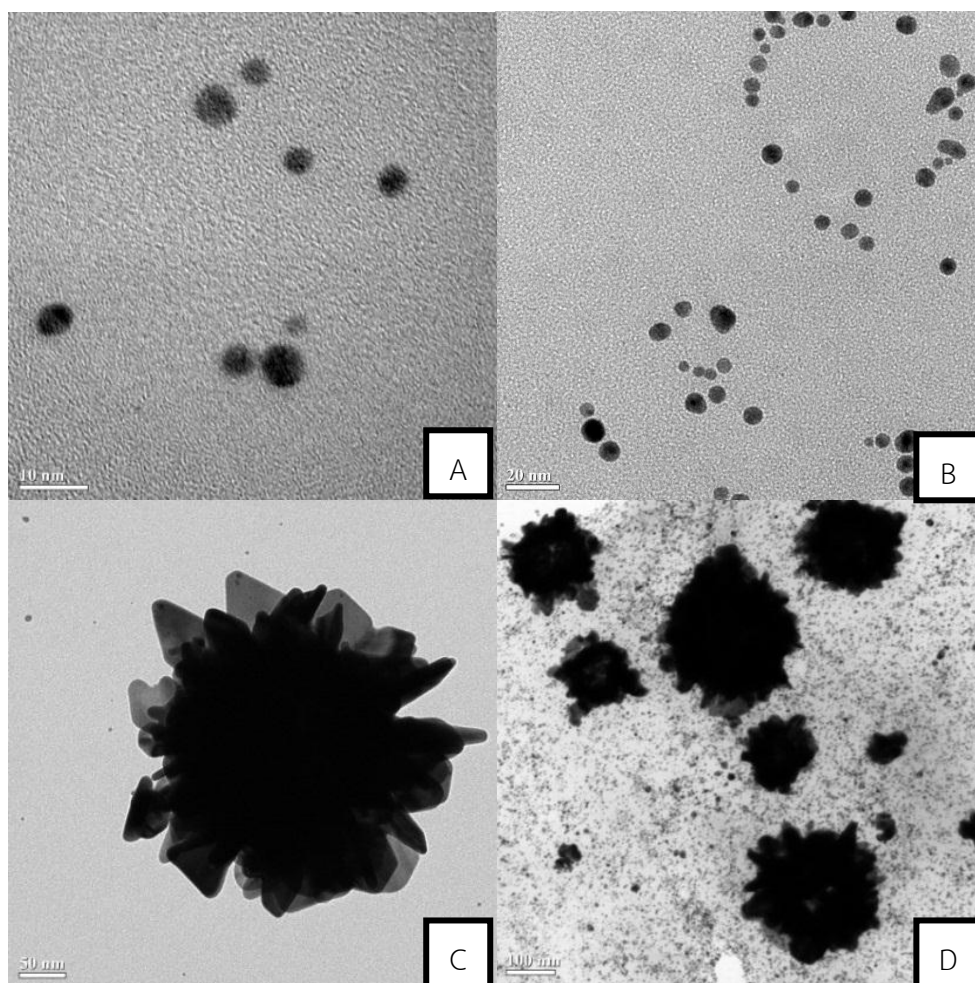
Figure 4.4: TEM images of (A-B) Au@P at 2% P, 150 µL of HAuCl$_4$, 100 µL (0.1 M NaOH); (C-D) polymer.

4.1.2.3 Energy Dispersive X-ray Spectrometry (EDX)

a. By SEM

The point-scan energy-dispersive X-ray spectroscopic analysis (EDS) spectrum for an ensemble of the Au@P shows a gold signal along with oxygen and carbon peaks, which may have originated from the biomolecules bound to the surface of the gold nanoparticles as shown in Figure 4.5. The results were indicated the particles composed of C, O as expected for pullulan. Si, Ca, Na, Mg, Al were also presented and they were from the glass substrates. The presence of Au was attributed to Au@P. A representative SEM image with corresponding EDS spot data,

was illustrated in the upset to Fig 4.5, which gave further evidence for the synthesized gold nanoparticles by identifying the distribution of C, O and Au in the cubic-like shape.
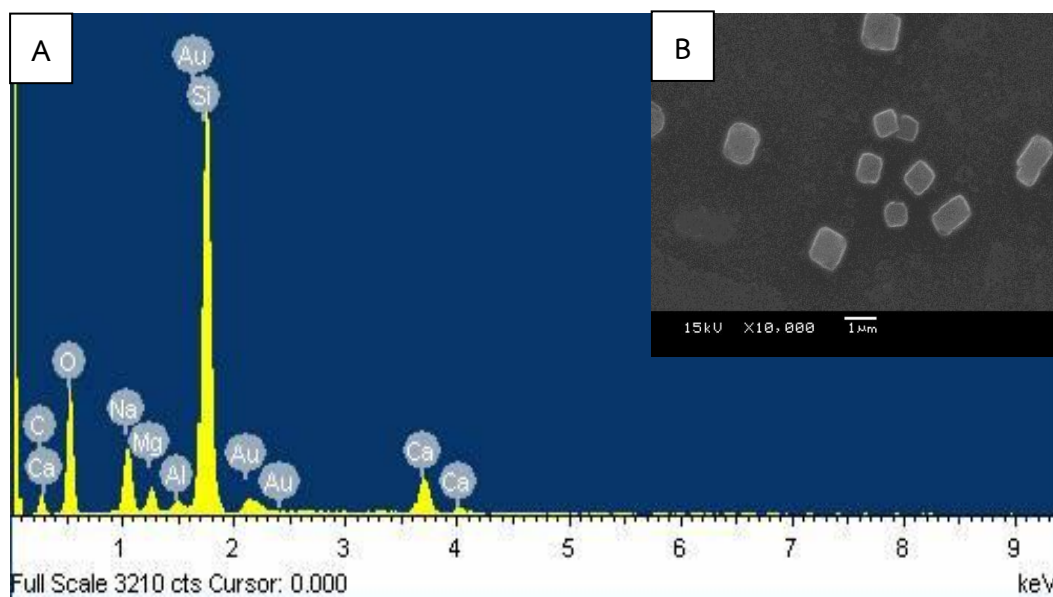
Figure 4.5: Characterization of the gold nanoparticles formed by the reaction of 150 µL of HAuCl$_4$ and 2% P at 80°C; (A) Spot profile EDS spectrum; (B) SEM images of Au@P.

b. By TEM

The spot profile EDS spectrum and TEM image recorded from the AuNPs are shown in Figure 4.6A and B, respectively. The EDS profile was shown a strong gold signal along with weak oxygen and strong carbon peaks, which may have originated from the biomolecules that were bound to the surface of the AuNPs. The TEM image was shown the spherical shape of AuNPs and an average size of 10 nm.
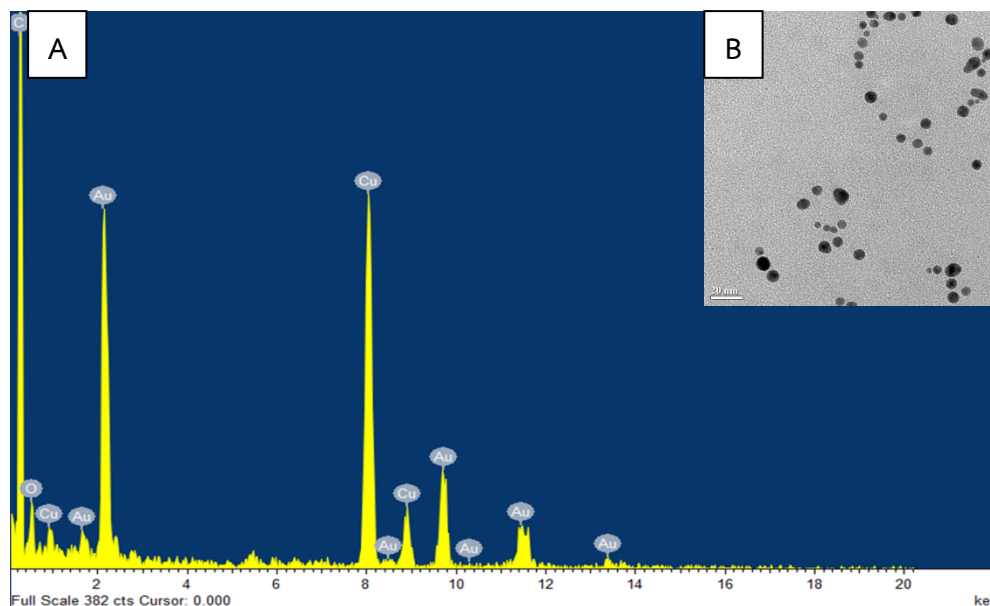
Figure 4.6: Characterization of the gold nanoparticles formed by the reaction of
150 µL of $HAuCl_4$ and 2%P at 80℃.; (A) Spot profile EDS spectrum; (B)
TEM images of Au@P.

4.1.3 Fourier-Transform Infrared Spectroscopy (FITR)

The strong absorption at 3320 cm^{-1} indicated that pullulan had some repeating units of –OH as in sugars. The other strong absorption at 2932 cm^{-1} indicated a C-H bond of alkane compounds. Further characteristic signals arrived at 1653, 1368 and 1153 cm^{-1} were due to C-O stretching, C-O-H bending and C-O-C stretching, respectively. The absorption peaks at 932 and 758 cm^{-1} demonstrated the linkage between glucose units were α-(1,4) and α-(1,6) linkage, 848 cm^{-1} characterized the α-configuration of α-D-glucopyranose units Similar results were reported in pullulan stabilized gold nanoparticles [31].
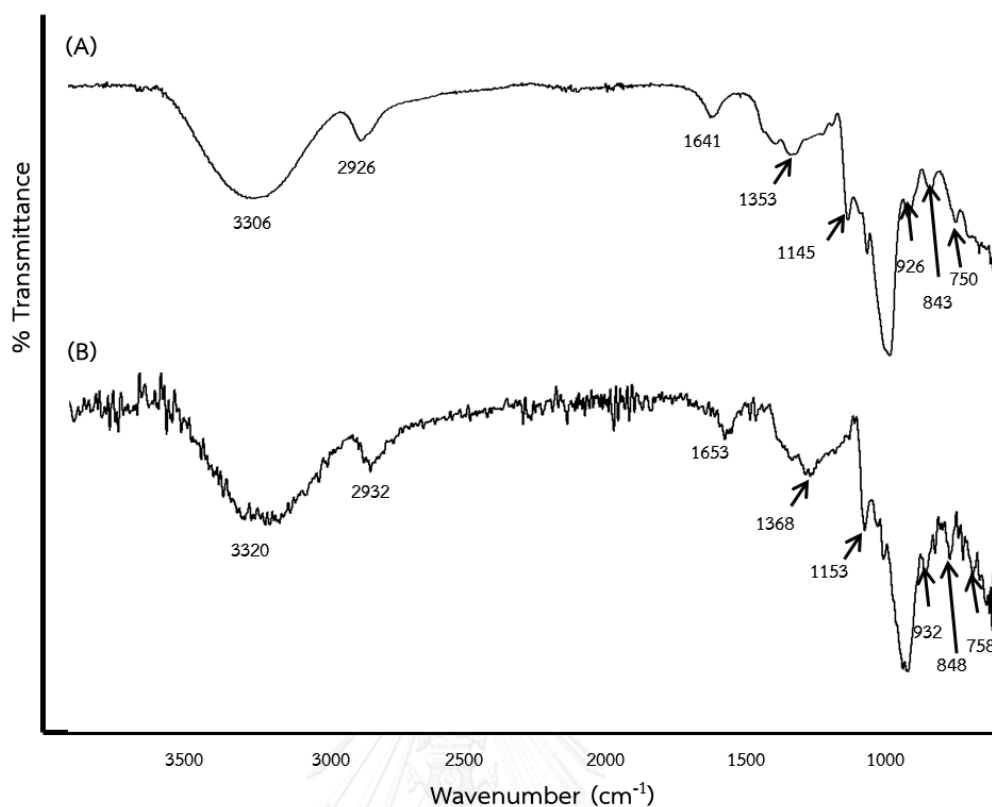
Figure 4.7: ATR-FTIR spectra of pullulan; (A) P; (B) Au@P.

4.2 Characterization of folic-acid-conjugated pullulan

4.2.1 Nuclear Magnetic Resonance (^{1}H-NMR)

The ^{1}H NMR spectra of folic acid (FA), pullulan (P) and pullulan-folic acid (P-FA) are shown in Figure.4.13, the internal standard used for assigning the chemical shifts of the protons were D_2O and DMSO, which appear as a singlet at 4.65 and 2.48 ppm, respectively.

The ^{1}H NMR spectrum of FA displayed the H7, H9 and H11 protons in aromatic ring at 8.63, 7.63 and 6.61 ppm, respectively. H8 and H10 protons in secondary amine (R_2NH) and amide (RCONHR') protons at 8.14 and 6.95 ppm, H12, H14-16 protons in methylene (CH_2) protons at 4.45, 2.29, 2.21 and 1.88 ppm, H13 protons in methine (CH) protons at 4.30 ppm were observed in Figure 4.13A.

The ^{1}H NMR spectrum of P was shown in Figure 4.13B, which revealed that the H1 protons of α-(1,4) and α-(1,6) linkage at 5.25 and 4.80 ppm , respectively were occurred. Furthermore, the characteristic peaks of H2-H6 showed at around 3.28-3.88 ppm. Moreover, Specific peaks of pullulan appeared between 3.0 ~ 5.8 ppm [45].

The ^{1}H NMR spectra of P-FA were observed the a-c protons of aromatic ring from FA on pullulan structure at 8.57, 7.50 and 6.63 ppm as shown in Figure 4.13C. Lee et al. showed the Specific peaks of folic acid appeared at 6.5 ~ 9.0 ppm [45]. Furthermore, the DS, as calculated from eq (1) using integration areas from ^{1}H NMR spectra was 6.39%.
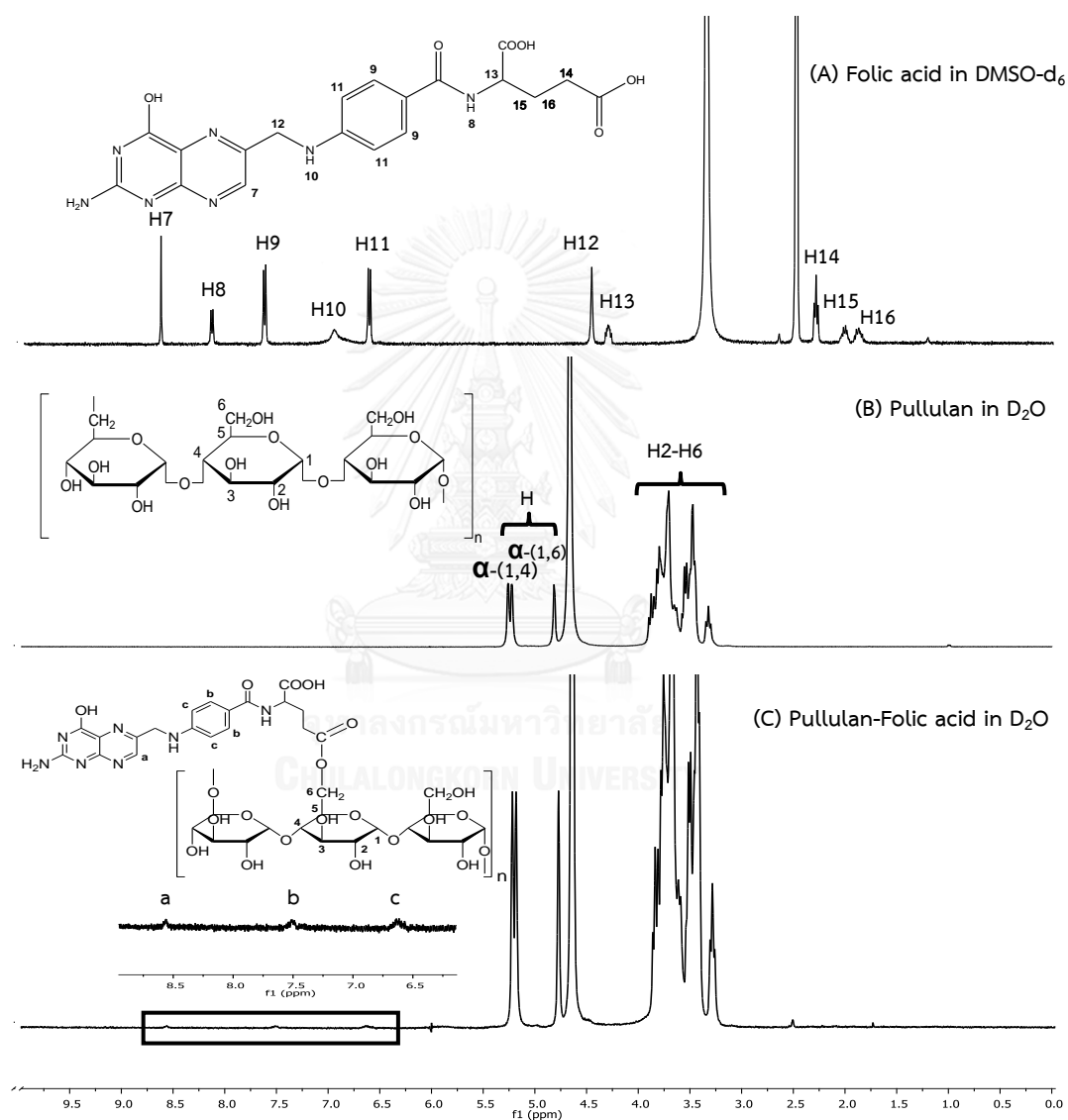
Figure 4.8: ^{1}H NMR spectra of (A) Folic acid in DMSO-d$_6$, (B) Pullulan in D$_2$O and (C) Folic acid with pullulan in D$_2$O

4.2.2 FTIR

The ATR-FTIR spectra, a broad band at 3306 cm^{-1} indicating –OH stretching of pullulan and other absorption at 2926 cm^{-1} was characteristic peak of C-H stretching as shown in Figure 4.14. Further characteristic signals at 1641, 1353 and 1145 cm^{-1} corresponded to O-C-O stretching, C-O-H bending and C-O-C stretching, respectively. The absorption peaks at 926 and 750 cm^{-1} demonstrated the linkage between glucose units were α-(1,4) and α-(1,6) linkage, 842 cm^{-1} characterized the α-configuration of α-D-glucopyranose units (Figure 4.14A).

The FTIR spectrum of FA (Figure 4.12B) represented the absorption peaks at 1685 cm^{-1} and 1603 cm^{-1} corresponding to C=O stretching and NH_2 bending vibration, respectively. Furthermore, the vibration at 1479 cm^{-1} was also observed related to phenyl ring (Figure 4.14B). In addition, Huang et al. showed The FTIR spectrum for folic acid. The spectrum for pure folic acid is characterized by a number of characteristic bands occurring at 1694, 1605 and 1484 cm^{-1}. The band at 1640 cm^{-1} belongs to the C-O bond stretching vibration of ⁻$CONH_2$ group. The band at 1605 cm^{-1} relates to the bending mode of NH-vibration and the band at 1484 cm^{-1} is attributed to characteristic absorption band of phenyl ring [51].

FTIR spectrum of P-FA was displayed a broad band appeared at 3303 cm^{-1} indicates that pullulan had some repeating units of –OH stretching, an absorption band at 1654 cm^{-1} due to stretching vibration from C-O and bending from –OH. The spectrum showed a peak at 1600 cm^{-1} due to bending vibration from NH_2 of FA, 1522 cm^{-1} due to phenyl ring (Figure 4.14C).
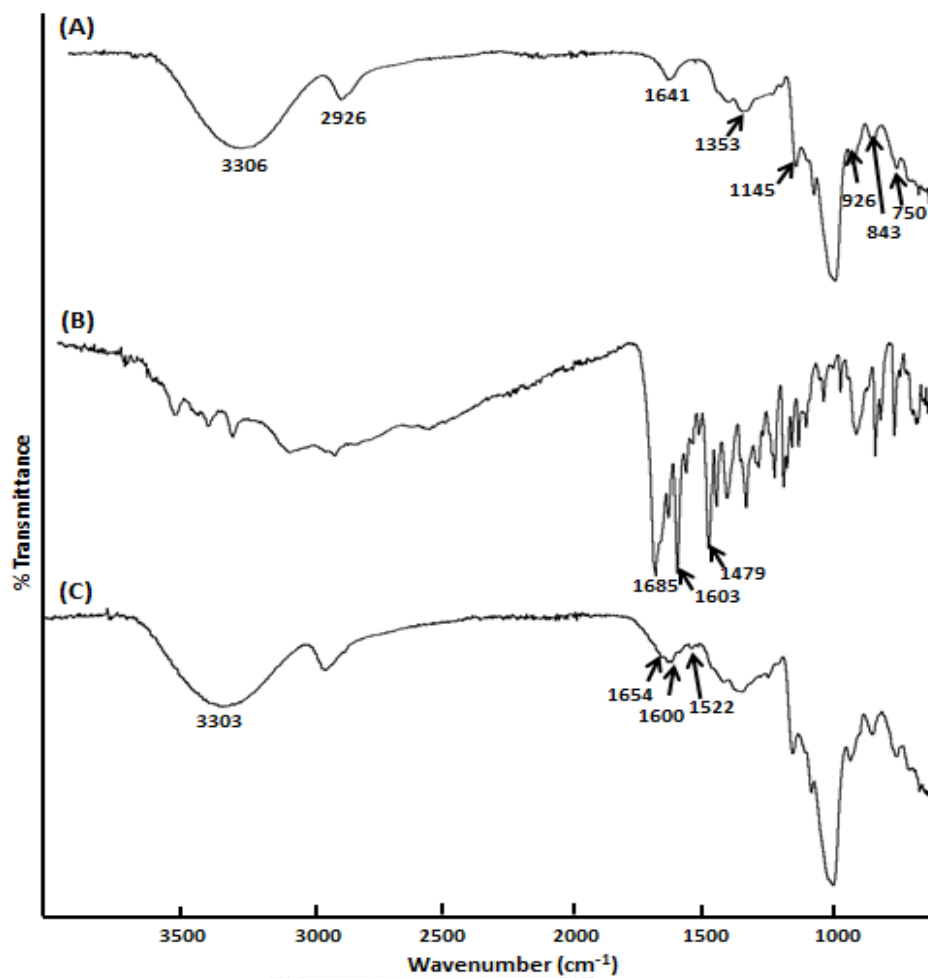
Figure 4.9: ATR-FTIR spectra of (A) Pullulan (P); (B) Folic acid (FA) and (C) P-FA

4.3 Synthesis and characterization of Au@P-FA

Folic acid is often selected for tumor targeting of drugs because most of tumor cells have numerous folate receptors on the cell surface [30]. Then, targeting to the folate receptor of tumor cells enables nanoparticles to concentrate anticancer drugs in tumor cells and to avoid healthy cells. Zwicke et al. introduced the folate receptor for active targeting of cancer cells using gold nanoparticles.

In this study, we used pullulan for conjugation of folic acid and fabrication of nanocarriers of the drug. The AuNPs production was monitored with the color change and UV–vis spectroscopy (Figure 4.8E). The reaction was started as soon as reagents were mixed, and the color of the mixture immediately changed from yellow (polymer color) to green.

4.3.1 Ultraviolet-visible (UV-vis) spectroscopy

The synthesized AuNPs using various concentrations of P-FA carried out in a mixture containing P-FA solution, NaOH and distilled water. The Au@P-FA at 150 µL of HAuCl$_4$, 100 µL (0.1 M NaOH), was the optimum condition with the maximum absorption of 0.7295 and the wavelength average remained at 600 nm. The solution turned to green under our conditions (Figure 4.9E). Zhang et al. presented the unmodified nanoparticles display a characteristic surface plasmon absorption at 520 nm and explained the red-shift of FA conjugated AuNPs band in the position of the maximum absorption indicates that FA has interacted with AuNPs [52]. It was studied on cytotoxicity by MTT assay.
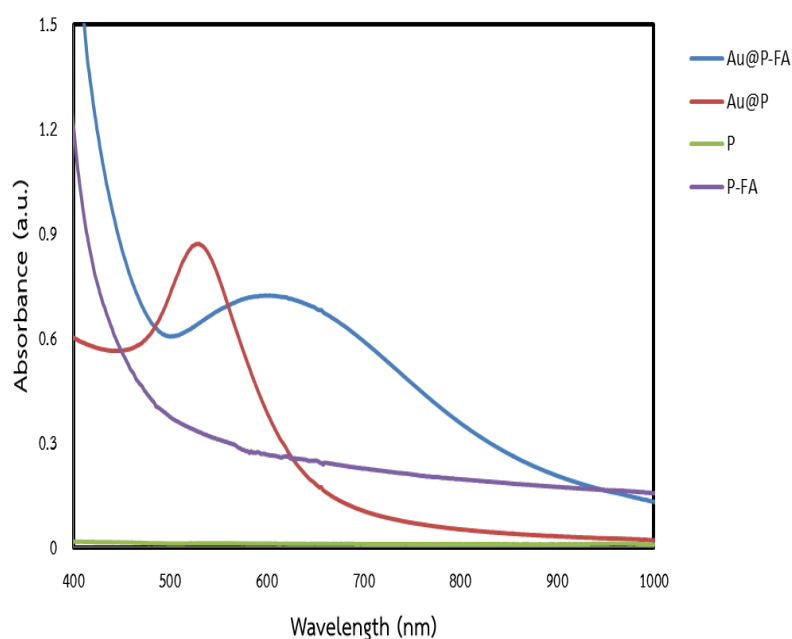
Figure 4.10: The absorption spectrum of Au@P and Au@P-FA were measured at wavelength range of 400-1000 nm on UV-vis spectrophotometer.
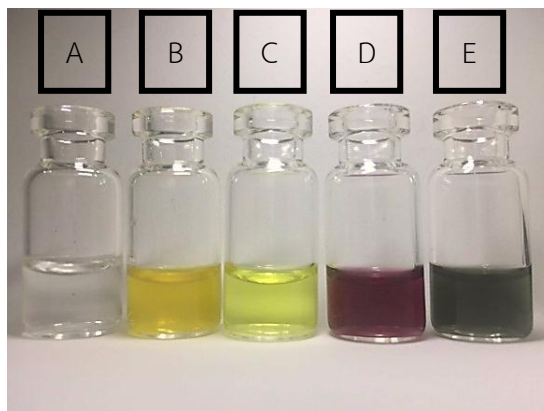
Figure 4.11: The color of mixture solution depending on our condition;
(A) 2% (w/v) of P; (B) 2% (w/v) of P-FA; (C) 10^3 ppm of $HAuCl_4$; (D) 2% P, 150 µL of $HAuCl_4$, 100 µL (0.1 M NaOH); (E) 2% P-FA, 150 µL of $HAuCl_4$, 100 µL (0.1 M NaOH).

4.3.2 Morphology of Au@P-FA

4.3.2.1 Scanning Electron Microscopy (SEM)

The SEM images of AuNPs prepared at 2%P-FA, 150 µL of $HAuCl_4$, 100 µL (0.1 M NaOH) were shown in Figure 4.10. The morphology of the particles was observed as a cubic-like structure. These structures were assembled by several particles. The particles are well dispersed and an average size of 1 µm. Therefore, the characterization of P-FA by TEM and EDS were not studied.
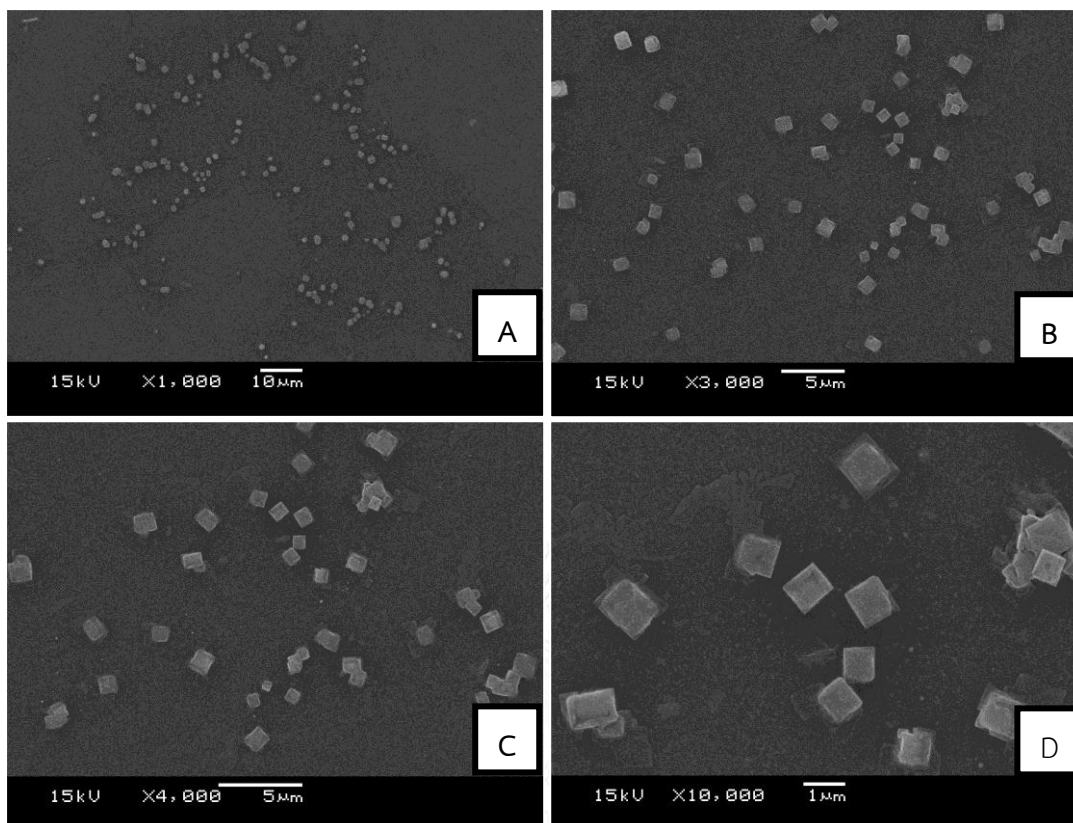
Figure 4.12: SEM images of Au@P-FA at 2% P-FA, 150 μL of HAuCl$_4$, 100 μL (0.1 M NaOH) 15 min; 1000X (A); 3000X (B); 4000X (C) and 10000X (D).

4.2.2.2 Energy Dispersive X-ray Spectrometry (EDS)

The spot-profile EDS spectrum of gold nanoparticles showed strong signals for gold atoms along with weak signal from carbon (Figure 4.11A). The results were indicated the particles composed of C, O as expected for pullulan. Si, Ca, Na, Mg, Al were also presented and they were occurred from the glass substrates. The presence of Au was attributed to Au@P-FA.
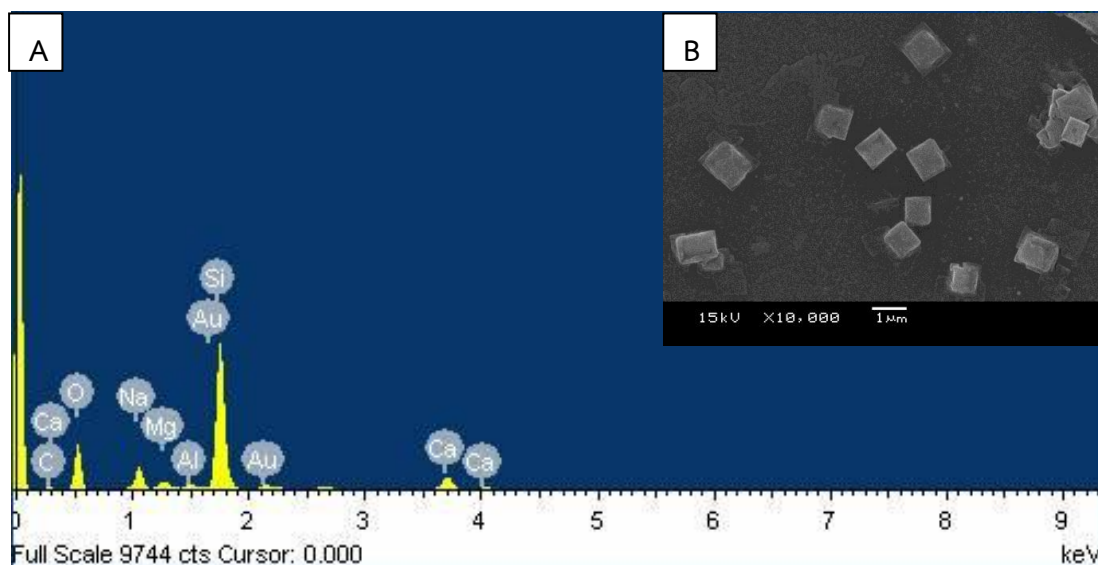
Figure 4.13: Characterization of the gold nanoparticles formed by the reaction of 0.5 mM $HAuCl_4$ and 2% P-FA at 80℃. (A) Spot profile EDS spectrum, (B) SEM images of Au@P-FA.

4.3.2.3 FITR of Au@P-FA

In pure FA (Figure 4.12B), the characteristic absorption peaks at 1410 cm^{-1} due to OH deformation of phenyl skeleton, 1479 cm^{-1} due to phenyl ring. 1603 cm^{-1} due to NH_2 bending vibration, 1685 cm^{-1} due to stretching vibration from –COOH, 2918, 2837 cm^{-1} due to symmetric stretching vibration of –CH_2, 3411, 3320 cm^{-1} due to stretching vibration of NH–H, 3544 cm^{-1} due to stretching vibration of OH were observed [51].

The FTIR spectrum of P-FA was displayed an absorption band at 1654 cm^{-1} due to stretching vibration from C-O and bending from –OH were observed in Figure 4.12C. The spectrum showed a peak at 1600 cm^{-1} due to bending vibration from NH_2 of FA, 1522 cm^{-1} due to phenyl ring (Figure 4.12C).

The FTIR (Figure 4.12D) spectrum of Au@P-FA was showed an absorption band at 1667 cm^{-1} due to the formation of amide bond between folic acid and pullulan.
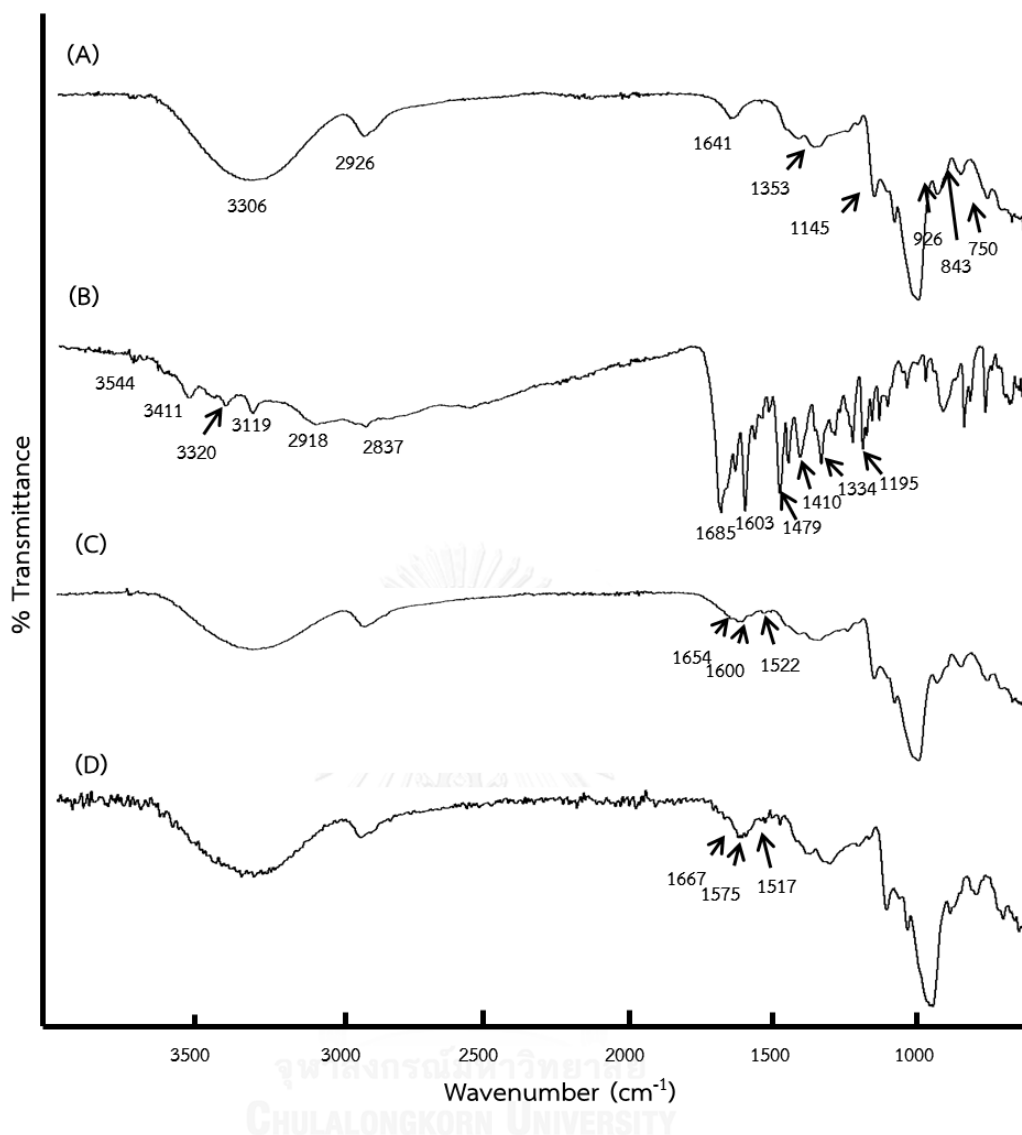
Figure 4.14: ATR-FTIR spectra of pullulan; (A) P; folic acid; (B) FA; (C) folic acid stabilized pullulan; P-FA; (D) gold nanoparticles stabilized pullulan-folic acid; Au@P-FA.

4.3 Biological activities

4.3.1 Effect of compounds on RAW 264.6 cells viability

In this study, we examined the effect of each compound on MTT assay for determination of cell viability at different concentrations. The RAW 264.7 cells line were treated with samples at various concentrations (Figure 4.15). Cell viability was measured by the activity of the mitochondrial dehydrogenases through the MTT assay.

The viability of RAW 264.7 cells in the present of budesonide (anti-inflammatory drug) and lycorine at a wide range of concentrations. The cell viability was estimated by MTT assay. As a result, the samples with concentration of 0.1-100 μM (cell viability >60%) of budesonide and 0.01-10 μM of lycorine, Ly+Au@P and Ly+Au@P-FA were selected for NO determination.

In addition, the results of the MTT assay demonstrated that exposure to increasing concentrations of Au@P and Au@P-FA resulted in no significant reduction in cell viability (≥80%cell viability). These data were indicated that treatment of Au@P and Au@P-FA did not affect cell viability or cell membrane integrity. Au@P and Au@P-FA did not produce a cytotoxic response after exposure for 24 h at various concentration (0.1–100 μM), which is consistent with other reported results in macrophages and human leukemia cells [53]. Besides, Cytotoxicity may not be the only adverse effect of nanoparticles; nanoparticles may also affect the immunological response of cells [54]. Shukla et al. tested the effect of gold nanoparticles on the proliferation, nitric oxide, and reactive oxygen species production of RAW264.7 macrophage cells. After 48 hours of up to 100 μM gold-nanoparticle treatment, RAW264.7 macrophage cells showed greater than 90% viability with no increase in pro-inflammatory cytokines [55].

In addition, the results suggested that the most of compounds do not affect the cell viability in activated RAW 264.7 cells on cytotoxicity activity (≥80% cell viability). Whereas the samples containing lycorine was showed high cytotoxicity against cancer cells line at 100 μM that was not selected for NO determination. Lin et al. presented the results on cytotoxicity. Lycorine was showed potent in vitro cytotoxicity [56] that could be a potential candidate to combat cancer cells [57]. Liu et al. demonstrated that lycorine displays higher in *vitro* growth inhibitory activity in human leukemic cells than in normal white blood cells [2].
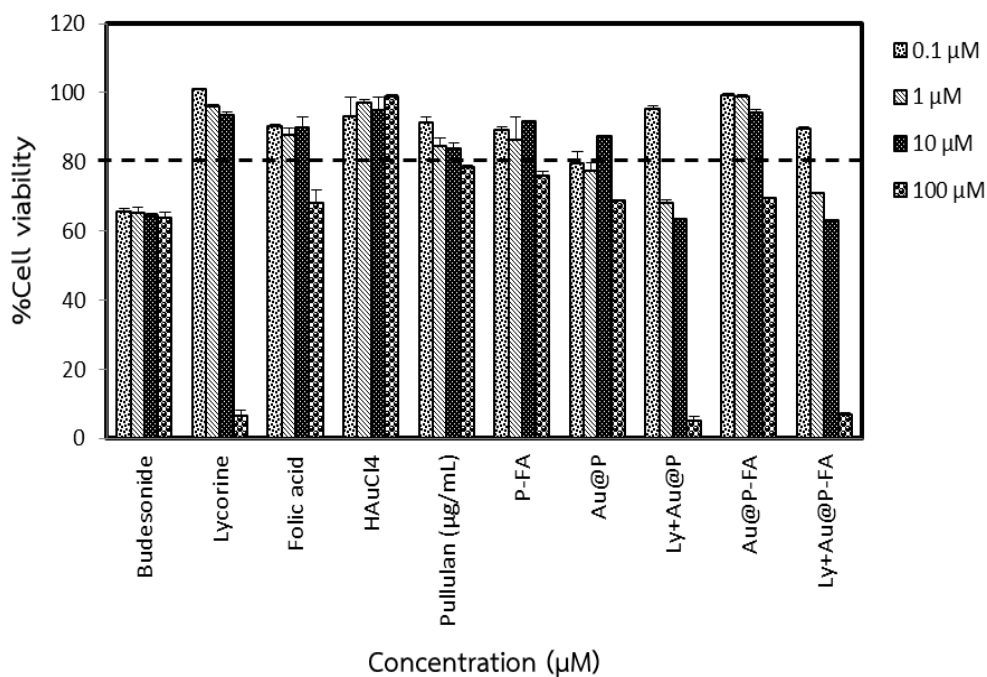
Figure 4.15: Cytotoxicity by MTT screening test of compounds against the murine macrophage leukemia cancer cells line (RAW 264.7 cells)

4.3.2 Effect of compounds on anti-inflammatory activity by nitric oxide (NO) inhibition.

In this study, we examined the effect of compounds on anti-inflammatory activity by nitric oxide inhibition at various concentrations of each substance (0-100 µM) on NO production from LPS-stimulated RAW 264.7 cell lines. Cell lines were treated with each compound at various concentrations with LPS for 24 h (Figure 4.13). The supernatants of macrophages treated with compounds for 24 h in the presence of LPS were used to measure nitrite formation, which serves as an indirect indicator of nitric oxide (NO) production.

To investigate NO production, nitrite (NO_2^-) from $NaNO_2$ was determined via reaction with Griess reagent and is measured since it is stable. The concentration of nitrite was measured by the absorbance at 540 nm and then It was calculated by $NaNO_2$ from calibration curve of nitrite standard, R^2 = 0.9982. The nitrite accumulation was significantly increased from RAW 264.7 cell lines by stimulation of LPS (1 µg/mL) when compared with control as shown in Figure 4.16.
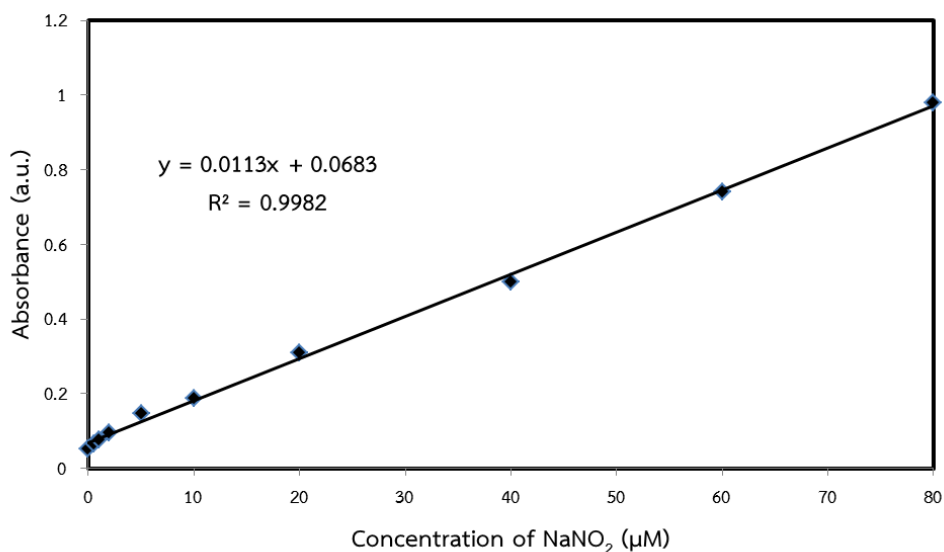
Figure 4.16: Calibration curve of nitrite standard

In this study, NO production of LPS stimulated RAW 264.7 cells line was inhibited by various concentrations of compounds which budesonide was used as a positive control. From the results shown in Figure 4.14, LPS can be stimulated inflammation higher 13.45 times than the control. Thus, LPS showed effectiveness to stimulate the inflammation. Furthermore, inflammation is a complex process involving multiple factors. The migration of leukocytes into the inflammation site is crucial for the pathogenesis of inflammatory conditions. The neutrophils and macrophages which are also known to play an important role in inflammation as pro-inflammatory cells induce the release of pro-inflammatory molecules such as tumor necrosis factor (TNF-α) and nitric oxide (NO) after activation [17].

From MTT assay, the viability of RAW 264.7 cells in the present of budenoside (anti-inflammatory drug) and lycorine at a wide range of concentrations (Figure 4.12). The cell viability was estimated by MTT assay. As a result, the samples containing budesonide do not effect on MTT assay. The RAW 264.7 cells were treated with budesonide at a various concentrations. It can be inhibits the NO production at concentration of 0.1-100 µM. The RAW 264.7 cells were treated with lycorine at a various concentrations. It can be inhibits the NO production at concentration of 10 µM. In this condition, RAW 264.7 cells were not inhibited 10 µg/mL of lycorine. According to inhibitory activity of lycorine on production of tumor necrosis factor

reported by Yui et al. could be also probably one of the mechanisms that responsible for the anti-inflammatory activity [58].

In the same way, the samples containing budesonide do not effect on MTT assay. The RAW 264.7 cells were treated with budesonide at a various concentrations. It can be inhibits the NO production at concentration of 10 µg/mL, however, in this condition, RAW 264.7 cells were not inhibit 10 µg/mL of budesonide.

The medium containing the concentration of folic acid and $HAuCl_4$ at 100 µM significantly inhibited RAW 264.7 cells on cytotoxicity activity. The medium containing the concentrations of Ly+Au@P at 10 µM significantly inhibited RAW 264.7 cells on cytotoxicity activity which is correspond with other reported results Au@P alone did not induce the release of nitric oxide from macrophages. Cells were treated with LPS as a positive control for NO production [53].

In the other hand, the medium containing the various concentrations of $HAuCl_4$, pullulan, P-FA and Au@P do not affect the NO production with LPS in RAW 264.7 cell lines at 100 µM because maybe cells were damaged or death or Samples have higher concentration that was interfered in supernatant (false positive). It makes the results too higher than control.
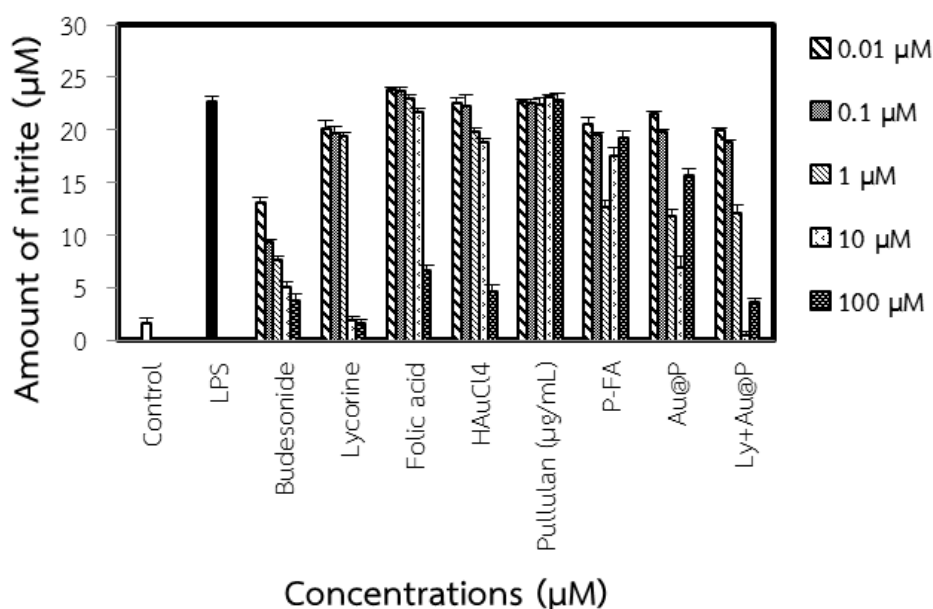
Figure 4.17: Nitrite content after inhibition with various concentration of each compound

4.4 Effects of the 2 agents applied separately and jointly with different concentrations

Effects increased as the concentration of the two agents were applied both separately and jointly, as shown in Table 1. Slope (m), median-effect (D_m) that is IC_{50}, and relative (r), is linear co-relation coefficient of the median-effect plot were worked out according to median-effect equation (Table 2). At 10 μM of Lycorine+Au@P, the combination index (CI) was calculated as 0.28879. The mutual effect of two agents were synergistic, D_m is 7.4423 μM and inhibition rate (*fa*) is 0.7666

Table 4.1: Effects (*fa*) of the 2 agents when applied separately and jointly at different concentrations (μM)

Drug concentration	lycorine		Au@P		Lycorine+Au@P	
0.01 μM	(20.2124)	0.083881	(21.7198)	0.018049	(20.0855)	0.075848
0.1 μM	(19.8584)	0.096714	(19.8938)	0.082629	(18.8997)	0.117788
1 μM	(19.4956)	0.716536	(16.9941)	0.185185	(12.2566)	0.352739
10 μM	(1.97050)	0.723526	(7.01180)	0.538237	(0.5546)	0.766615
100 μM	(1.77286)	0.730725	(15.7168)	0.23036	(3.7434)	0.653834

Table 4.2: Slope, median-effect concentration and relative ratio when the 2 agents are applied separately and jointly.

Drug	Slope (m)	median-effect concentration (D_m)	relative ratio (r)
lycorine	0.4332	2.2303	0.8787
Au@P	0.3536	157.0100	0.8369
Lycorine+Au@P	0.4114	7.4423	0.9327

Table 4.3: Ratio relationship of drug concentrations (μM) when the 2 drugs are jointly applied.

Drug concentration	lycorine	Au@P	fa	CI
0.01 μM	20.2124	21.7198	0.0759	1.4770
0.1 μM	19.8584	19.8938	0.1178	4.7758
1 μM	19.4956	16.9941	0.3527	1.8383
10 μM	1.97050	7.01180	0.7666	0.2890
100 μM	1.77286	15.7168	0.6538	10.3820

CHAPTER V

CONCLUSION

To conclude, the GNPs were produced by the use of pullulan as reducing and stabilizing agent. In this study, this method is green and environmentally friendly. Thus, the synthesized AuNPs could have a high potential for use in biological applications. This method is inexpensive and highly recommended to be used in large-scale production of AuNPs.

In this research, the Au@P was successfully synthesized. The finally solution turned to red under our conditions. The morphology of synthesized AuNPs by a range of techniques including scanning electron microscopy (SEM) and transmission electron microscopy (TEM). The SEM images of AuNPs was prepared at 2%P and 2% P-FA, 150 μL of $HAuCl_4$. The shape of the particles was observed as a cubic-like structure. The particles are well dispersed and an average size of 1 μm. Therefore, the higher concentration of pullulan was not studied. We characterized by TEM technigue to confirmed size distribution for synthesis of Au@P. It has a particles size about 10 nm. The shape of Au@P is spherical shape.

In addition, the P-FA was successfully synthesized. The degree substitution of P-FA was calculated using integration areas from ^{1}H NMR spectra was 6.39%. The ATR-FTIR spectrum of P-FA was presented a broad band appeared at 3303 cm^{-1} indicates that pullulan had some repeating units of –OH stretching, an absorption band at 1654 cm^{-1} due to stretching vibration from C-O and bending from –OH. The spectrum showed a peak at 1600 cm^{-1} due to bending vibration from NH_2 of FA, 1522 cm^{-1} due to phenyl ring.

Moreover, we examined the effect of each compounds on MTT assay for determination of cell viability at different concentrations. Cell viability was measured by the activity of the mitochondrial dehydrogenases through the MTT assay. As a result, the samples with concentration of 0.1-100 μM (cell viability >60%) of budesonide and 0.01-10 μM (cell viability >80%) of lycorine and ly+Au@P were selected for NO determination. The results of the MTT assay demonstrated that exposure to increasing concentrations of Au@P resulted in no significant reduction in cell viability (≥80%cell viability). The results suggested that the most of compounds do not affect the cell viability in activated RAW 264.7 cells on cytotoxicity activity

The present study has demonstrated that Au@P were internalized by cultured macrophages but exhibited no cytotoxicity and proinflammatory responses at

concentrations ranging from of 0.1–10 mg/ml. These biocompatible characteristics make Au@P promising candidates for biomedical applications in drug delivery.

Finally, NO production of LPS stimulated RAW 264.7 cells line was inhibited by various concentrations of compounds, budesonide was used as a positive control. The RAW 264.7 cells were treated with budesonide at a various concentrations. It can be inhibits the NO production at concentration of 0.1-100 µM. The RAW 264.7 cells were treated with lycorine at a various concentrations. It can be inhibits the NO production at concentration of 10 µg/mL. The RAW 264.7 cells were treated with budesonide at a various concentrations. In the other hand, the medium containing the various concentrations of $HAuCl_4$, pullulan and P-FA do not affect the NO production with LPS in RAW 264.7 cells line. The medium containing the concentrations of folic acid and Au@P at 100 µM significantly inhibited RAW 264.7 cells on cytotoxicity activity which is correspond with other reported results Au@P alone did not induce the release of nitric oxide from macrophages.

The results demonstrated that 10 µM of Ly+Au@P could inhibit similar to budesonide (control anti-inflammatory drug) in NO production. This work showed a successful inhibition agent derived from the excellent combination of Ly+Au@P. The combination index (CI) of Ly+Au@P was 0.28897 (synergistic) at 10 µM Cells were treated with LPS as a positive control for NO production.

lycorine-Au@P is a good therapeutic candidate against inflammation which can inhibit the expression of cytokines.

จุฬาลงกรณ์มหาวิทยาลัย
CHULALONGKORN UNIVERSITY

REFERENCES

[1]   Wellen, K.E., Hotamisligil, G., xF, and khan, S. Inflammation, stress, and diabetes. The Journal of Clinical Investigation 115(5): 1111-1119.

[2]   Liu, X.-s., Jiang, J., Jiao, X.-y., Wu, Y.-e., Lin, J.-h., and Cai, Y.-m. Lycorine induces apoptosis and down-regulation of Mcl-1 in human leukemia cells. Cancer Letters 274(1) (2009): 16-24.

[3]   Chen, H., Dorrigan, A., Saad, S., Hare, D.J., Cortie, M.B., and Valenzuela, S.M. In Vivo Study of Spherical Gold Nanoparticles: Inflammatory Effects and Distribution in Mice. PLoS ONE 8(2) (2013): e58208.

[4]   BarathManiKanth, S., et al. Anti-oxidant effect of gold nanoparticles restrains hyperglycemic conditions in diabetic mice. Journal of Nanobiotechnology 8(1) (2010): 1-15.

[5]   Hickey, T., Kreutzer, D., Burgess, D.J., and Moussy, F. Dexamethasone/PLGA microspheres for continuous delivery of an anti-inflammatory drug for implantable medical devices. Biomaterials 23(7) (2002): 1649-1656.

[6]   Wallace, J.L., Ferraz, J.G.P., and Muscara, M.N. Hydrogen Sulfide: An Endogenous Mediator of Resolution of Inflammation and Injury. Antioxidants & Redox Signaling 17(1) (2011): 58-67.

[7]   Pattison, D.J. and Winyard, P.G. Dietary antioxidants in inflammatory arthritis: do they have any role in etiology or therapy? Nat Clin Pract Rheum 4(11) (2008): 590-596.

[8]   BERENBAUM, F. Free radicals and inflammation. Annals of the Rheumatic Diseases 60(5) (2001): 442.

[9]   Serhan, C.N., et al. Resolution of inflammation: state of the art, definitions and terms. The FASEB Journal 21(2) (2007): 325-332.

[10]   Frölich, L. and Riederer, P. Free radical mechanisms in dementia of Alzheimer type and the potential for antioxidative treatment. Arzneimittel-Forschung 45(3A) (1995): 443-446.

[11]   Elgorashi, E.E., Stafford, G.I., and van Staden, J. Acetylcholinesterase Enzyme Inhibitory Effects of Amaryllidaceae Alkaloids. Planta Med 70(03) (2004): 260-262.

[12]   Neurath, M.F. Cytokines in inflammatory bowel disease. Nat Rev Immunol 14(5) (2014): 329-342.

[13]   Ilavenil, S., et al. Hepatoprotective mechanism of lycorine against carbon tetrachloride induced toxicity in swiss albino mice – A proteomic approach. Asian Pacific Journal of Reproduction 4(2) (2015): 123-128.

[14]   Vrijsen, R., Vanden Berghe, D.A., Vlietinck, A.J., and Boeyé, A. Lycorine: a eukaryotic termination inhibitor? Journal of Biological Chemistry 261(2) (1986): 505-507.

[15]   Mikami, M., et al. Suppressive Activity of Lycoricidinol (Narciclasine) against Cytotoxicity of Neutrophil-Derived Calprotectin, and Its Suppressive Effect on Rat A djuvant Arthritis Model. Biological & Pharmaceutical Bulletin 22(7) (1999): 674-678.

[16]   Kim, Y.H., et al. Anti-inflammatory activity of Crinum asiaticum Linne var. japonicum extract and its application as a cosmeceutical ingredient. Journal of cosmetic science 59(5) (2008): 419-430.

[17]   Saltan Çitoğlu, G., Bahadır Acıkara, Ö., Sever Yılmaz, B., and Özbek, H. Evaluation of analgesic, anti-inflammatory and hepatoprotective effects of lycorine from Sternbergia fisheriana (Herbert) Rupr. Fitoterapia 83(1) (2012): 81-87.

[18]   Kang, J., et al. Lycorine inhibits lipopolysaccharide-induced iNOS and COX-2 up-regulation in RAW264.7 cells through suppressing P38 and STATs activation and increases the survival rate of mice after LPS challenge. International Immunopharmacology 12(1) (2012): 249-256.

[19]   Pirlamarla, P. and Bond, R.M. FDA labeling of NSAIDs: Review of nonsteroidal anti-inflammatory drugs in cardiovascular disease. Trends in Cardiovascular Medicine 26(8) (2016): 675-680.

[20] Moran, A.P. Lipopolysaccharide in bacterial chronic infection: Insights from Helicobacter pylori lipopolysaccharide and lipid A. International Journal of Medical Microbiology 297(5) (2007): 307-319.

[21] Ohmori, Y. and Hamilton, T.A. Requirement for STAT1 in LPS-induced gene expression in macrophages. Journal of Leukocyte Biology 69(4) (2001): 598-604.

[22] Tewtrakul, S. and Subhadhirasakul, S. Effects of compounds from Kaempferia parviflora on nitric oxide, prostaglandin E2 and tumor necrosis factor-alpha productions in RAW264.7 macrophage cells. Journal of Ethnopharmacology 120(1) (2008): 81-84.

[23] Spoelstra, F.M., Postma, D.S., Hovenga, H., Noordhoek, J.A., and Kauffman, H.F. Additive anti-inflammatory effect of formoterol and budesonide on human lung fibroblasts. Thorax 57(3) (2002): 237-241.

[24] Mendes, E.S., Rebolledo, P., Campos, M., and Wanner, A. Immediate Antiinflammatory Effects of Inhaled Budesonide in Patients with Asthma. Annals of the American Thoracic Society 11(5) (2014): 706-711.

[25] Gibson, P.G., Saltos, N., and Fakes, K. Acute Anti-inflammatory Effects of Inhaled Budesonide in Asthma. American Journal of Respiratory and Critical Care Medicine 163(1) (2001): 32-36.

[26] Fact sheet N°297 [Online] 2015. Available from: http://www.who.int/mediacentre/factsheets/fs297/en/

[27] Snyder, I.S. and Stringer, J.L. Anticancer drug [Online] Available from: https://global.britannica.com/science/anticancer-drug

[28] Dhamecha, D., Jalalpure, S., Jadhav, K., Jagwani, S., and Chavan, R. Doxorubicin loaded gold nanoparticles: Implication of passive targeting on anticancer efficacy. Pharmacological Research 113, Part A (2016): 547-556.

[29] Pistone, A., et al. Tunable doxorubicin release from polymer-gated multiwalled carbon nanotubes. International Journal of Pharmaceutics 515(1–2) (2016): 30-36.

[30] Zwicke, G.L., Mansoori, G.A., and Jeffery, C.J. Utilizing the folate receptor for active targeting of cancer nanotherapeutics. 2012 (2012).

[31]   Ganeshkumar, M., Ponrasu, T., Raja, M.D., Subamekala, M.K., and Suguna, L. Green synthesis of pullulan stabilized gold nanoparticles for cancer targeted drug delivery. <u>Spectrochimica Acta Part A: Molecular and Biomolecular Spectroscopy</u> 130 (2014): 64-71.

[32]   Ghosh, P., Han, G., De, M., Kim, C.K., and Rotello, V.M. Gold nanoparticles in delivery applications. <u>Adv Drug Deliv Rev</u> 60(11) (2008): 1307-1315.

[33]   França, A., Aggarwal, P., Barsov, E.V., Kozlov, S.V., Dobrovolskaia, M.A., and González-Fernández, Á. Macrophage scavenger receptor A mediates the uptake of gold colloids by macrophages in vitro. <u>Nanomedicine</u> 6(7) (2011): 1175-1188.

[34]   Sumbayev, V.V., et al. Gold Nanoparticles Downregulate Interleukin-1β-Induced Pro-Inflammatory Responses. <u>Small</u> 9(3) (2013): 472-477.

[35]   Beitollahi, H., Ivari, S.G., and Torkzadeh-Mahani, M. Voltammetric determination of 6-thioguanine and folic acid using a carbon paste electrode modified with ZnO-CuO nanoplates and modifier. <u>Materials Science and Engineering: C</u> 69 (2016): 128-133.

[36]   Low, P.S., Henne, W.A., and Doorneweerd, D.D. Discovery and Development of Folic-Acid-Based Receptor Targeting for Imaging and Therapy of Cancer and Inflammatory Diseases. <u>Accounts of Chemical Research</u> 41(1) (2008): 120-129.

[37]   Emwas, A.-H.M., J.S. Merzaban, and H. Serrai. <u>Chapter 3 - Theory and Applications of NMR-Based Metabolomics in Human Disease Diagnosis A2 - ur-Rahman, Atta.</u> Applications of NMR Spectroscopy. Vol. 1, 2015.

[38]   Movasaghi, Z., Rehman, S., and ur Rehman, D.I. Fourier Transform Infrared (FTIR) Spectroscopy of Biological Tissues. <u>Applied Spectroscopy Reviews</u> 43(2) (2008): 134-179.

[39]   Giordano, M., Kansiz, M., Heraud, P., Beardall, J., Wood, B., and McNaughton, D. FOURIER TRANSFORM INFRARED SPECTROSCOPY AS A NOVEL TOOL TO INVESTIGATE CHANGES IN INTRACELLULAR MACROMOLECULAR POOLS IN THE MARINE MICROALGA CHAETOCEROS MUELLERII (BACILLARIOPHYCEAE). <u>Journal of Phycology</u> 37(2) (2001): 271-279.

[40] Yang, Y., et al. Inhibition of nitric oxide synthesis delayed mature-green tomato fruits ripening induced by inhibition of ethylene. Scientia Horticulturae 211 (2016): 95-101.

[41] Kim, H.K., Cheon, B.S., Kim, Y.H., Kim, S.Y., and Kim, H.P. Effects of naturally occurring flavonoids on nitric oxide production in the macrophage cell line RAW 264.7 and their structure-activity relationships. Biochem Pharmacol 58(5) (1999): 759-65.

[42] Lee, M., Lee, Y., Soltermann, F., and von Gunten, U. Analysis of N-nitrosamines and other nitro(so) compounds in water by high-performance liquid chromatography with post-column UV photolysis/Griess reaction. Water Research 47(14) (2013): 4893-4903.

[43] Ramos, L.A., Cavalheiro, C.C.S., and Cavalheiro, É.T.G. Determinação de nitrito em águas utilizando extrato de flores. Química Nova 29 (2006): 1114-1120.

[44] in Sittampalam, G.S., et al. (eds.),Assay Guidance Manual. Bethesda (MD): Eli Lilly & Company and the National Center for Advancing Translational Sciences, 2004.

[45] Lee, S.J., Shim, Y.-H., Oh, J.-S., Jeong, Y.-I., Park, I.-K., and Lee, H.C. Folic-acid-conjugated pullulan/poly(DL-lactide-co-glycolide) graft copolymer nanoparticles for folate-receptor-mediated drug delivery. Nanoscale Research Letters 10(1) (2015): 1-11.

[46] Yang, E.-J., Yim, E.-Y., Song, G., Kim, G.-O., and Hyun, C.-G. Inhibition of nitric oxide production in lipopolysaccharide-activated RAW 264.7 macrophages by Jeju plant extracts. in Interdisciplinary Toxicology. 2009. 245.

[47] Chou, T.C. Drug combination studies and their synergy quantification using the Chou-Talalay method. Cancer Res 70(2) (2010): 440-6.

[48] He, S., Shen, W., and Shen, D.-m. Application of median-effect in quantitative analysis of antitumor drugs in vitro. Chinese Journal of Cancer Research 17(2) (2005): 140-144.

[49] Shankar, S.S., Rai, A., Ahmad, A., and Sastry, M. Rapid synthesis of Au, Ag, and bimetallic Au core–Ag shell nanoparticles using Neem (Azadirachta indica) leaf broth. Journal of Colloid and Interface Science 275(2) (2004): 496-502.

[50]   Dixit, V., Van den Bossche, J., Sherman, D.M., Thompson, D.H., and Andres, R.P. Synthesis and Grafting of Thioctic Acid–PEG–Folate Conjugates onto Au Nanoparticles for Selective Targeting of Folate Receptor-Positive Tumor Cells. Bioconjugate Chemistry 17(3) (2006): 603-609.

[51]   Huang, H., Yuan, Q., Shah, J.S., and Misra, R.D. A new family of folate-decorated and carbon nanotube-mediated drug delivery system: synthesis and drug delivery response. Adv Drug Deliv Rev 63(14-15) (2011): 1332-9.

[52]   Zhang, Z., Jia, J., Lai, Y., Ma, Y., Weng, J., and Sun, L. Conjugating folic acid to gold nanoparticles through glutathione for targeting and detecting cancer cells. Bioorganic & Medicinal Chemistry 18(15) (2010): 5528-5534.

[53]   Zhang, Q., Hitchins, V.M., Schrand, A.M., Hussain, S.M., and Goering, P.L. Uptake of gold nanoparticles in murine macrophage cells without cytotoxicity or production of pro-inflammatory mediators. Nanotoxicology 5(3) (2011): 284-95.

[54]   Lewinski, N., Colvin, V., and Drezek, R. Cytotoxicity of Nanoparticles. Small 4(1) (2008): 26-49.

[55]   Shukla, R., Bansal, V., Chaudhary, M., Basu, A., Bhonde, R.R., and Sastry, M. Biocompatibility of gold nanoparticles and their endocytotic fate inside the cellular compartment: a microscopic overview. Langmuir 21(23) (2005): 10644-54.

[56]   Lin, L.-Z., et al. Lycorine alkaloids from Hymenocallis littoralis. Phytochemistry 40(4) (1995): 1295-1298.

[57]   Lamoral-Theys, D., et al. Lycorine, the Main Phenanthridine Amaryllidaceae Alkaloid, Exhibits Significant Antitumor Activity in Cancer Cells That Display Resistance to Proapoptotic Stimuli: An Investigation of Structure–Activity Relationship and Mechanistic Insight. Journal of Medicinal Chemistry 52(20) (2009): 6244-6256.

[58]   Yui, S., Mikami, M., Kitahara, M., and Yamazaki, M. The inhibitory effect of lycorine on tumor cell apoptosis induced by polymorphonuclear leukocyte-derived calprotectin. Immunopharmacology 40(2) (1998): 151-162.

APPENDIX A

Absorbance of synthesis of gold nanoparticles using pullulan and P-FA
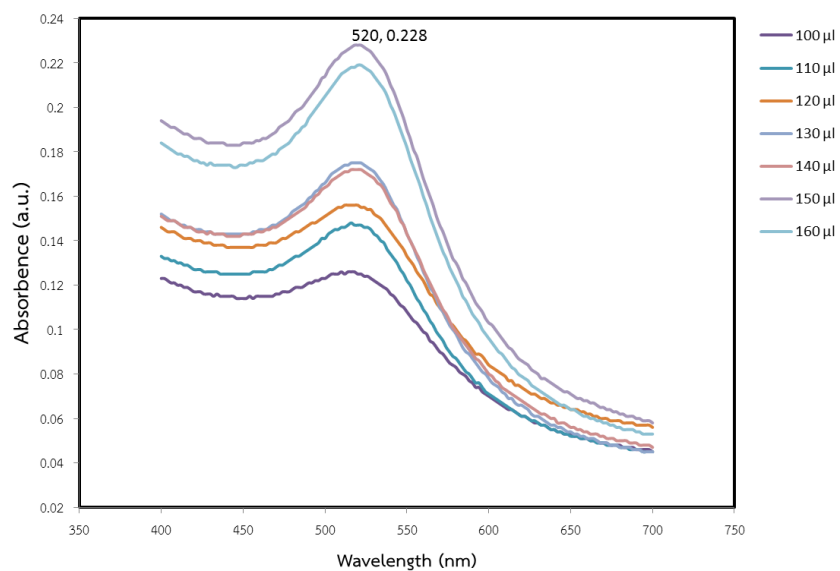
Figure A1: The absorption spectra of Au@P were measured at wavelength range of 400-700 nm on microtiter plate reader; various volumes of $HAuCl_4$.
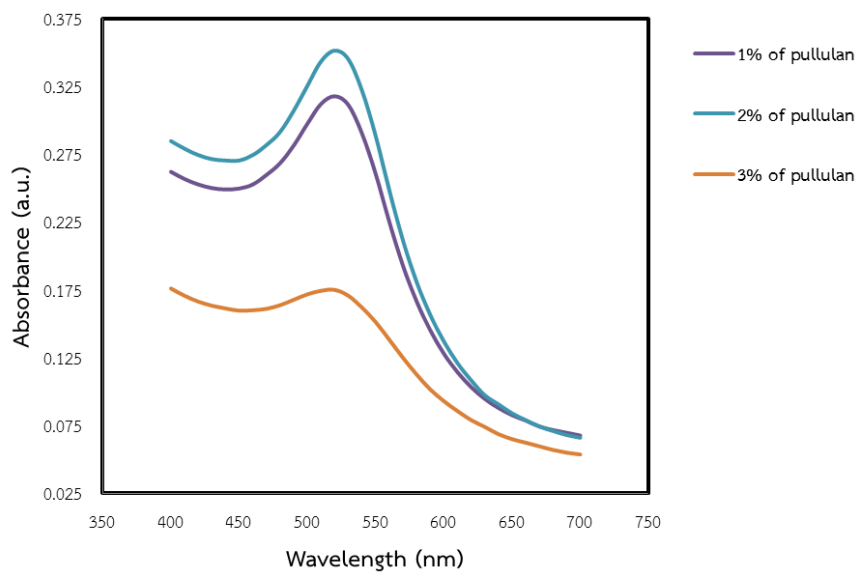
Figure 2A: The absorption spectrum of Au@P with various concentrations of pullulan were measured at wavelength range of 400-700 nm on microtiter plate reader
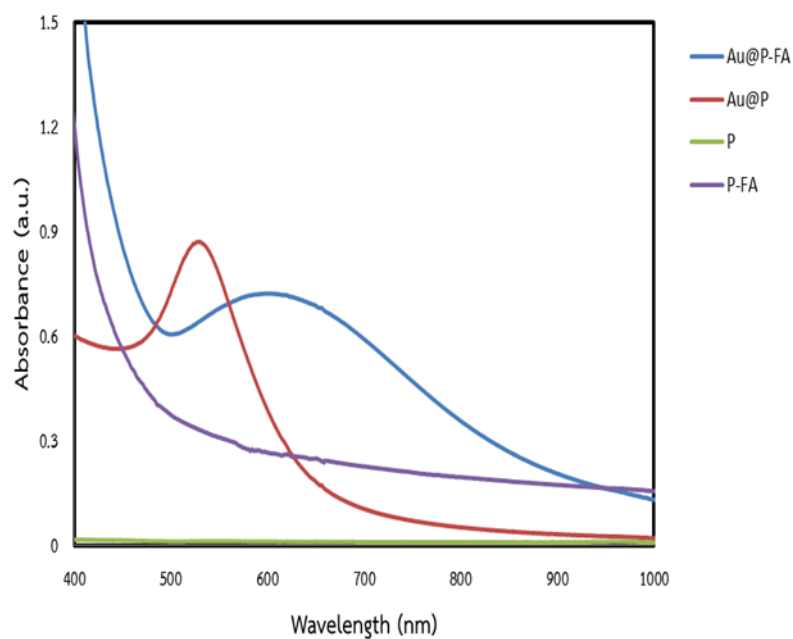
Figure 3A: The absorption spectrum of Au@P and Au@P-FA were measured at wavelength range of 400-700 nm on microtiter plate reader; various concentrations of pullulan

APPENDIX B

Characterizations of pullulan-folic acid

56
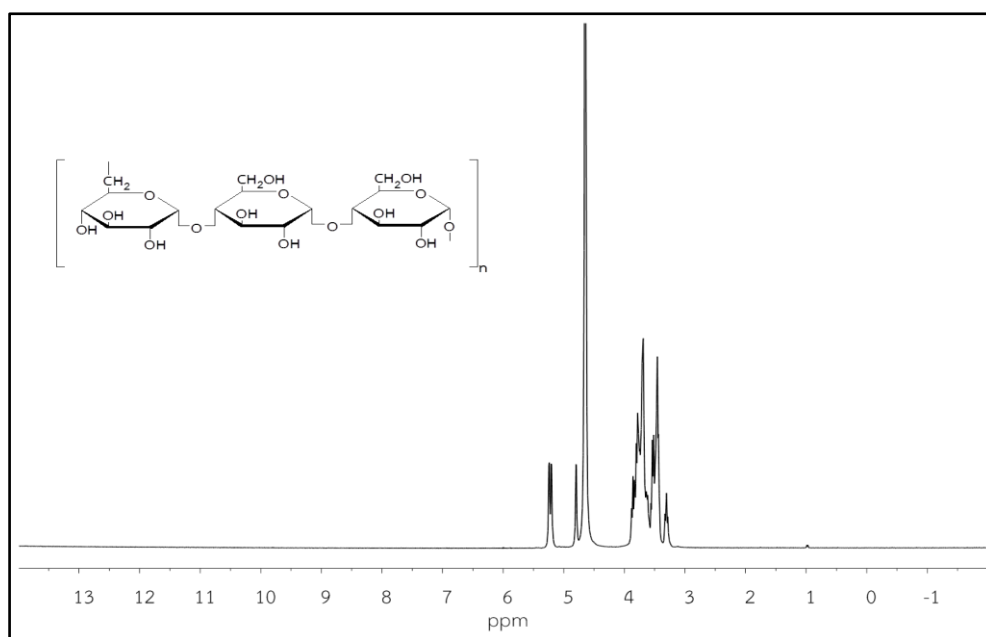
Figure A4: ^{1}H-NMR spectrum of pullulan in D$_2$O
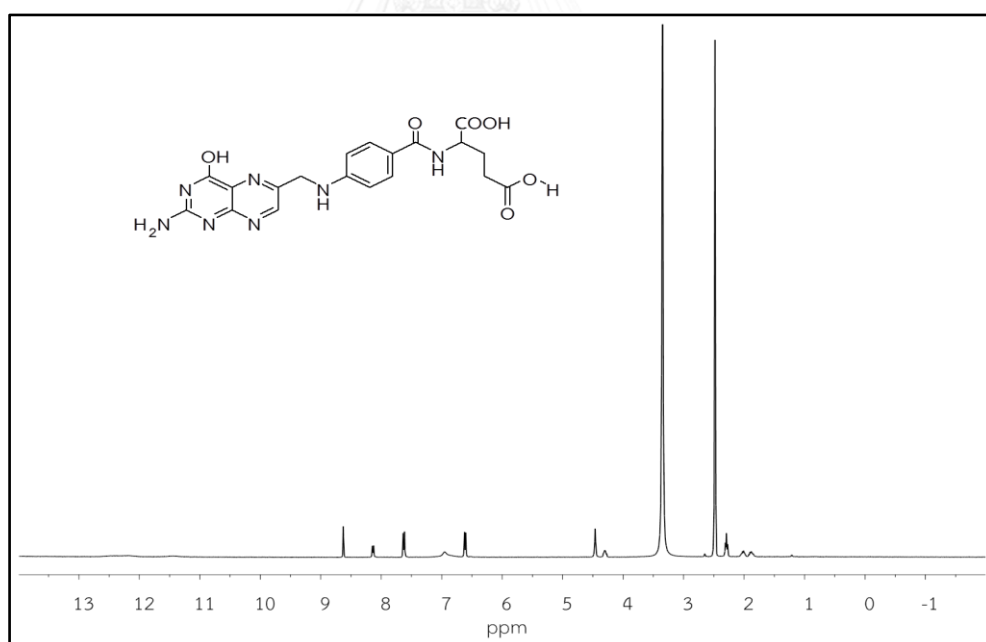
Figure A5: ^{1}H-NMR spectrum of folic acid in DMSO-d$_6$
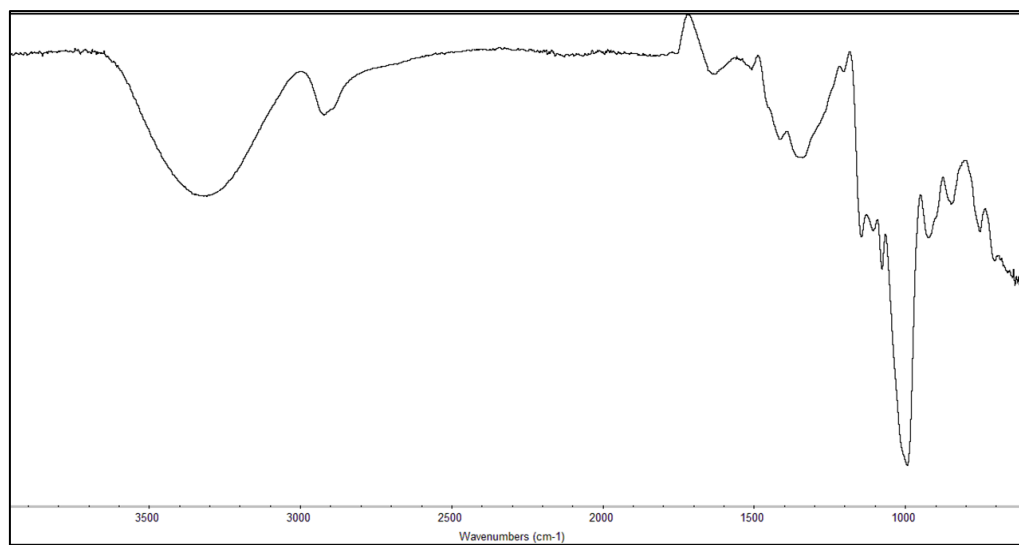
Figure A6: FTIR spectrum of pullulan
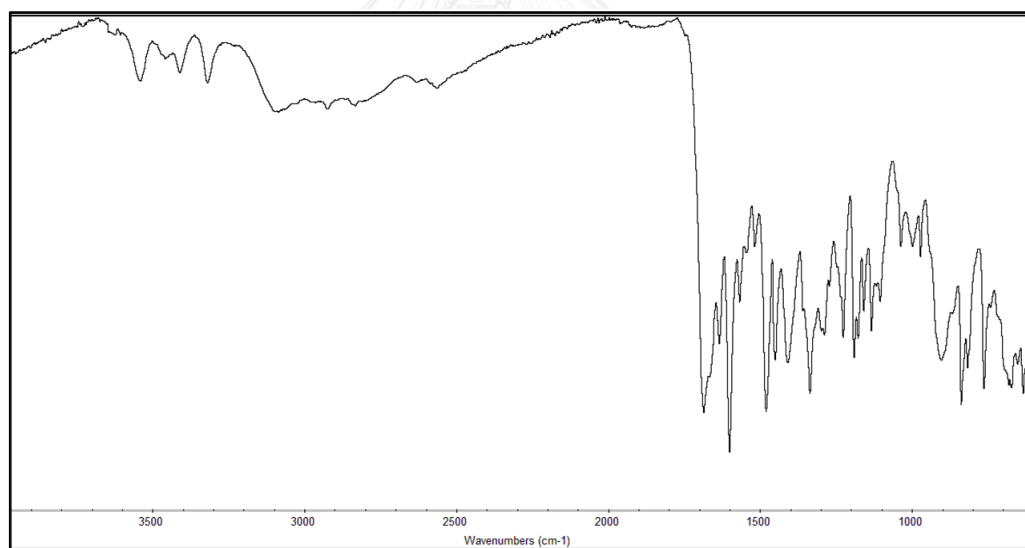
Figure A7: FTIR spectrum of folic acid

APPENDIX C

The degree substitution of pullulan-folic acid

The Determination of degree of substitution (%DS) on P-FA by ^{1}H NMR was measured the degree of substitution (DS) of Folic acid in P-FA, which is one of the important characteristics of P-FA. The DS was calculated using the data obtained from the ^{1}H NMR spectra according to:

$$\%DS = \left[\frac{(ArH)}{(H1)}\right] \times \frac{1}{5} \times 100$$

Where (ArH) is the integration area of Aromatic at 8.57, 7.50 and 6.63 ppm, respectively and (H1) is the integration area of α-(1,4) and α-(1,6) linkage of pullulan at (5.22,5.18) and 4.77 ppm, respectively.

From ^{1}H NMR spectrum of P-FA

$$\%DS = \left[\frac{(0.47)}{(1.47)}\right] \times \frac{1}{5} \times 100$$

$$\%DS = \frac{0.3197}{5} \times 100$$

$$\%DS = 6.39$$

APPENDIX D
Biological assays

Table 1D: Absorbance of each compound on cytotoxicity by MTT assay determined in 540 nm

Concentration(μM)	Budesonide				
	Abs [*]	Abs	Abs	AVG [**]	SD [***]
100	2.3963	2.3287	-	2.3625	0.0478
10	2.3641	2.2179	2.1210	2.2343	0.12238
1	2.3388	2.3875	2.3134	2.3466	0.037656
0.1	2.4218	2.4355	2.2454	2.3676	0.106021
0.01	2.5109	2.3474	2.1649	2.3411	0.173087
Concentration(μM)	Lycorine				
	Abs	Abs	Abs	AVG	SD
100	1.2980	1.1804	1.2218	1.2334	0.0597
10	2.0559	1.9038	2.0714	2.0104	0.0926
1	1.9758	2.0599	2.0885	2.0414	0.0586
0.1	2.3178	2.0208	2.2069	2.1818	0.1501
0.01	2.5641	2.3568	2.3123	2.4111	0.1344
Concentration(μM)	Folic acid				
	Abs	Abs	Abs	AVG	SD
100	2.7569	2.3758	2.1316	2.4214	0.315138
10	2.4790	2.2960	2.3383	2.3711	0.095808
1	2.4681	2.3778	2.3240	2.3900	0.072816
0.1	2.3714	2.3512	2.2663	2.3296	0.05577
0.01	2.3217	2.4624	2.1694	2.3178	0.146538
Concentration(μM)	Chloroauric acid (HAuCl$_4$)				
	Abs	Abs	Abs	AVG	SD
100	1.8488	1.7785	1.9550	1.8608	0.088856
10	2.0492	2.1276	2.0401	2.0723	0.048107
1	1.9426	2.2512	2.2592	2.1510	0.180524
0.1	2.1297	2.3529	2.4779	2.3202	0.176393
0.01	2.1918	2.1420	2.1228	2.1522	0.035613

[*] Abs = Absorbance

[**] AVG = Average

[***] SD = Standard deviation

Table 1D: Absorbance of each compound on cytotoxicity by MTT assay determined in 540 nm (cont.)

Concentration(µM)	Pullulan (P)				
	Abs [*]	Abs	Abs	AVG [**]	SD [***]
100	2.0830	2.2553	2.5130	2.2838	0.216409
10	2.1565	2.1684	2.0080	2.1110	0.08937
1	2.2326	2.0730	1.9656	2.0904	0.134348
0.1	2.4685	2.4417	2.4257	2.4453	0.021626
0.01	2.2051	2.6714	2.6600	2.5122	0.265989
Concentration(µM)	Pullulan-Folic acid (P-FA)				
	Abs	Abs	Abs	AVG	SD
100	2.0209	1.9988	1.9959	2.0052	0.013674
10	2.1042	2.2344	2.2094	2.1827	0.069094
1	2.1514	2.2138	2.2907	2.2186	0.069776
0.1	2.1308	2.2489	2.2962	2.2253	0.085188
0.01	2.3181	2.2186	2.3968	2.3112	0.089302
Concentration (µM)	Au@P				
	Abs	Abs	Abs	AVG	SD
100	1.8475	1.6879	1.6336	1.7230	0.1112
10	1.8588	2.0918	1.9783	1.9763	0.1165
1	1.7022	2.6204	2.0546	2.1257	0.4632
0.1	1.6423	1.8731	2.3877	1.9677	0.3816
0.01	1.9337	2.0189	2.4863	2.1463	0.2975
Concentration (µM)	Lycorine+Au@P				
	Abs	Abs	Abs	AVG	SD
100	0.9254	0.8536	0.8067	0.8619	0.059784
10	2.4853	2.6027	2.5627	2.5502	0.059685
1	2.2830	2.2427	2.1975	2.2411	0.042773
0.1	2.0855	2.3455	2.3163	2.2491	0.142432
0.01	2.2668	2.2953	2.2302	2.2641	0.032634

[*] Abs = Absorbance

[**] AVG = Average

[***] SD = Standard deviation

Table 2D: %Cell viability of each compound on cytotoxicity by MTT assay
determined in 540 nm.

Concentration(μM)	Budesonide				
	%[*]	%	%	AVG %[**]	SD %[***]
100	97.7789	95.02054	-	96.3997	1.950454
10	96.465	90.49944	86.54552	91.1700	4.993621
1	95.43266	97.41982	94.39624	95.7496	1.536503
0.1	98.8194	99.37842	91.62156	96.6065	4.326091
0.01	102.455	95.78357	88.33682	95.5251	7.062658
Concentration(μM)	Lycorine				
	%	%	%	AVG %	SD %
100	52.96374	48.16518	49.85447	50.3278	2.4340
10	83.88918	77.68287	84.52164	82.0312	3.7790
1	-	84.05239	85.21939	84.6359	0.8252
0.1	94.57577	-	90.0506	92.3132	3.1998
0.01	-	96.16713	94.35135	95.2592	1.2840
Concentration(μM)	Folic acid				
	%	%	%	AVG %	SD %
100	-	92.85607	83.31173	88.0839	6.748871
10	-	89.73716	91.39042	90.56379	1.16903
1	-	92.93424	90.83151	91.88288	1.486852
0.1	92.6841	91.8946	-	92.28935	0.55826
0.01	90.74162	96.24076	-	93.49119	3.888477
Concentration(μM)	Chloroauric acid (HAuCl$_4$)				
	%	%	%	AVG %	SD %
100	72.25874	69.51112	76.40947	72.72644	3.472876
10	80.0912	-	79.73553	79.91336	0.251494
1	-	87.98619	88.29886	88.14253	0.221093
0.1	83.23747	91.96105	-	87.59926	6.168501
0.01	85.66459	83.7182	82.96779	84.11686	1.3919

[*] % = %cell viability

[**] AVG % = Average of %cell viability

[***] SD % = Standard deviation of %cell viability

Table 2D: %Cell viability of each compound on cytotoxicity by MTT assay determined in 540 nm (cont.).

Concentration(μM)	Pullulan (P)				
	%[*]	%	%	AVG %[**]	SD %[***]
100	83.86344	90.80039	-	87.33191	4.905165
10	86.82261	87.30172	-	87.06216	0.338778
1	89.88646	83.46083	-	86.67365	4.543612
0.1	99.38401	98.30502	97.66084	98.44996	0.870678
0.01	-	107.5529	107.094	107.3235	0.324544

Concentration(μM)	Pullulan-Folic acid (P-FA)				
	%	%	%	AVG %	SD %
100	81.36323	80.47347	80.35671	80.73114	0.550515
10	84.71697	89.95893	88.95241	87.8761	2.781795
1	86.61728	89.12956	92.22562	89.32415	2.80923
0.1	-	90.54272	92.44706	91.49489	1.346572
0.01	93.32877	-	96.4973	94.91304	2.240491

Concentration(μM)	Au@P				
	%	%	%	AVG %	SD %
100	74.99721	68.51842	66.31418	69.94327	4.513469
10	75.45592	84.9143	80.30689	80.2257	4.729711
1	69.09892	-	83.4042	76.25156	10.11536
0.1	66.66734	76.03641	-	71.35188	6.624933
0.01	78.4964	81.955	-	80.2257	2.445599

Concentration(μM)	Lycorine+Au@P				
	%	%	%	AVG %	SD %
100	-	34.65094	32.74709	33.69902	1.346228
10	-	105.6537	104.03	104.8418	1.148169
1	92.67585	91.03991	89.20507	90.97361	1.736338
0.1	-	95.21297	94.02762	94.62029	0.838163
0.01	92.01823	93.17515	90.53249	91.90862	1.324736

[*] % = %cell viability

[**] AVG % = Average of %cell viability

[***] SD % = Standard deviation of %cell viability

Table 3D: Absorbance of $NaNO_2$ in DMEM medium determined in 540 nm

Concentration (µM)	Abs	Abs	Abs	AVG	SD
0	0.05	0.0541	0.0503	0.05147	0.0023
0.5	0.0631	0.0653	0.0641	0.06417	0.0011
1.0	0.0776	-	0.0745	0.0761	0.0338
2.0	0.0959	0.0945	0.0932	0.0945	0.0014
5.0	0.1481	0.1498	0.1435	0.1471	0.0033
10.0	0.1856	0.1882	0.1903	0.1880	0.0024
20.0	0.3061	0.3113	0.3094	0.3089	0.0026
40.0	0.4969	0.4987	0.4992	0.4983	0.0012
60.0	0.7474	0.7348	0.7424	0.7415	0.0063
80.0	0.9797	0.9813	0.9751	0.9787	0.0032
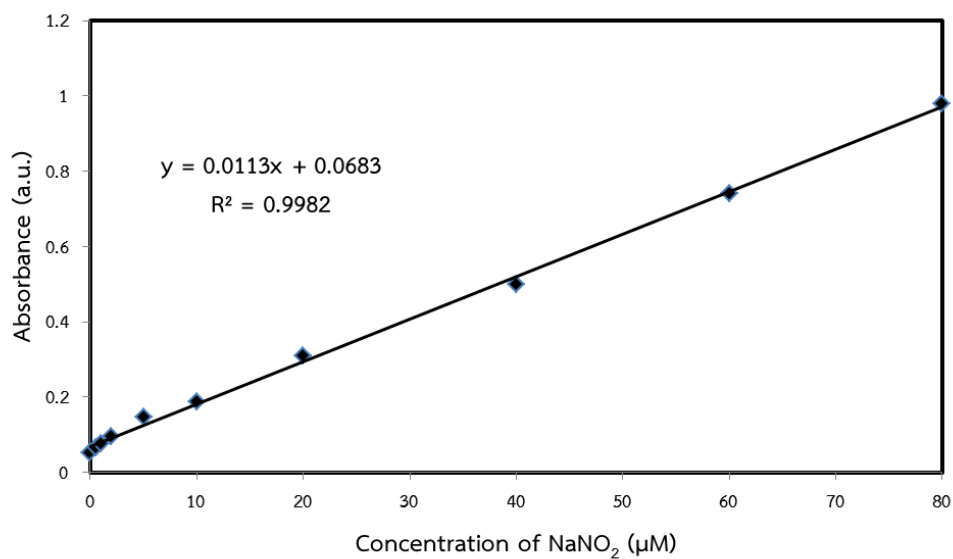
Figure 1D: Calibration curve of nitrite standard at concentration of 0-80 µM

Table 4D: Absorbance of each compounds on anti-inflammatory activity determined in 540 nm

Concentration(μM)	Budesonide				
	Abs [*]	Abs	Abs	AVG [**]	SD [***]
100	0.1178	0.106	0.112	0.111933	0.0059
10	0.1288	0.1217	0.1297	0.126733	0.004382
1	0.1512	0.1571	0.1579	0.1554	0.003659
0.1	0.1765	0.1744	0.1747	0.1752	0.001136
0.01	0.2182	0.2136	0.2211	0.217633	0.003782
Concentration(μM)	Lycorine				
	Abs	Abs	Abs	AVG	SD
100	0.0863	0.0908	0.0879	0.088333	0.002281
10	0.0876	0.0898	0.0943	0.090567	0.003415
1	0.2896	0.2903	0.2859	0.2886	0.002364
0.1	0.2917	0.2881	0.2983	0.2927	0.005173
0.01	0.2884	0.2965	0.3052	0.2967	0.008402
Concentration(μM)	Folic acid				
	Abs	Abs	Abs	AVG	SD
100	0.1405	0.1484	0.1454	0.144767	0.003988
10	0.3179	0.3129	0.3114	0.314067	0.003403
1	0.3271	0.3304	0.3324	0.329967	0.002676
0.1	0.3401	0.3334	0.3374	0.336967	0.003371
0.01	0.3398	0.3388	0.3381	0.3389	0.000854
Concentration(μM)	Chloroauric acid ($HAuCl_4$)				
	Abs	Abs	Abs	AVG	SD
100	0.118	0.1193	0.1288	0.122033	0.005896
10	0.2802	0.2847	0.2816	0.282167	0.002303
1	0.2938	0.2972	0.2907	0.2939	0.003251
0.1	0.3137	0.3365	0.3256	0.325267	0.011404
0.01	0.3234	0.3176	0.3232	0.3214	0.003292

[*] Abs = Absorbance

[**] AVG = Average

[***] SD = Standard deviation

Table 4D: Absorbance of each compounds on anti-inflammatory activity determined
in 540 nm (cont.)

Concentration(µM)	Pullulan (P)				
	Abs[*]	Abs	Abs	AVG[**]	SD[***]
100	0.3275	0.3346	0.3223	0.328133	0.006174
10	0.3299	0.3323	0.3297	0.330633	0.001447
1	0.3301	0.3178	0.3213	0.323067	0.006337
0.1	0.3275	0.3259	0.3222	0.3252	0.002718
0.01	0.3273	0.3238	0.3256	0.325567	0.00175
Concentration(µM)	Pullulan-Folic acid (P-FA)				
	Abs	Abs	Abs	AVG	SD
100	0.2857	0.2939	0.2813	0.286967	0.006395
10	0.2626	0.2619	0.2773	0.267267	0.008696
1	0.208	0.2109	0.2184	0.212433	0.005367
0.1	0.2925	0.2894	0.2903	0.290733	0.001595
0.01	0.2987	0.2992	0.3094	0.302433	0.006038
Concentration(µM)	Au@P				
	Abs	Abs	Abs	AVG	SD
100	0.2414	0.2504	0.3122	0.2459	0.038542
10	0.1354	0.1543	-	0.147533	0.013364
1	0.2548	0.2639	0.2623	0.260333	0.004858
0.1	0.2955	0.291	0.2928	0.2931	0.002265
0.01	0.3145	0.3138	0.3129	0.313733	0.000802
Concentration(µM)	Lycorine+Au@P				
	Abs	Abs	Abs	AVG	SD
100	0.1087	0.1102	0.1129	0.1106	0.002128
10	0.0776	0.0716	0.0745	0.074567	0.003001
1	0.2091	0.1996	0.2117	0.2068	0.006369
0.1	0.2763	0.2862	0.2831	0.281867	0.005064
0.01	0.2971	0.2929	0.2958	0.295267	0.00215

[*] Abs = Absorbance

[**] AVG = Average

[***] SD = Standard deviation

Table 5D: Nitric oxide contents of each compounds on anti-inflammatiory activity determined in 540 nm.

Concentration(μM)	Budesonide				
	NO[*]	NO	NO	AVG NO[**]	SD NO[***]
100	4.380531	3.336283	3.867257	4.380531	0.522149
10	5.353982	4.725664	5.433628	5.353982	0.387802
1	7.336283	7.858407	7.929204	7.336283	0.323826
0.1	9.575221	9.389381	9.415929	9.575221	0.100512
0.01	13.26549	12.85841	13.52212	13.26549	0.334688
Concentration(μM)	Lycorine				
	NO	NO	NO	AVG NO	SD NO
100	1.59292	1.99115	1.734513	1.772861	0.201866
10	1.707965	1.902655	2.300885	1.970501	0.302227
1	19.58407	19.64602	19.25664	19.49558	0.209232
0.1	19.76991	19.45133	20.35398	19.85841	0.457788
0.01	19.47788	20.19469	20.9646	20.21239	0.743521
Concentration(μM)	Folic acid				
	NO	NO	NO	AVG NO	SD NO
100	6.389381	7.088496	6.823009	6.766962	0.352911
10	22.0885	21.64602	21.51327	21.74926	0.301188
1	22.90265	23.19469	23.37168	23.15634	0.236853
0.1	24.0531	23.46018	23.81416	23.77581	0.298315
0.01	24.02655	23.93805	23.87611	23.9469	0.075611
Concentration(μM)	Chloroauric acid (HAuCl$_4$)				
	NO	NO	NO	AVG NO	SD NO
100	4.39823	4.513274	5.353982	4.755162	0.521774
10	18.75221	19.15044	18.87611	18.92625	0.203796
1	19.95575	20.25664	19.68142	19.9646	0.287713
0.1	21.71681	23.73451	22.76991	22.74041	1.009173
0.01	22.57522	22.06195	22.55752	22.39823	0.291364

[*] NO = Amount of nitrite

[**] AVG NO = Average of nitrite

[***] SD NO = Standard deviation of nitrite

Table 5D: Nitric oxide contents of each compounds on anti-inflammatiory activity determined in 540 nm (cont.)

Concentration(µM)	Pullulan (P)				
	NO [*]	NO	NO	AVG NO [**]	SD NO [***]
100	22.93805	23.56637	22.47788	22.9941	0.546408
10	23.15044	23.36283	23.13274	23.21534	0.128039
1	23.16814	22.07965	22.38938	22.54572	0.560837
0.1	22.93805	22.79646	22.46903	22.73451	0.240571
0.01	22.92035	22.61062	22.76991	22.76696	0.154888
Concentration(µM)	Pullulan-Folic acid (P-FA)				
	NO	NO	NO	AVG NO	SD NO
100	19.23894	19.9646	18.84956	19.35103	0.565911
10	17.19469	17.13274	18.49558	17.60767	0.769572
1	12.36283	12.61947	13.28319	12.75516	0.474945
0.1	19.84071	19.56637	19.64602	19.68437	0.141131
0.01	20.38938	20.43363	21.33628	20.71976	0.534379
Concentration(µM)	Au@P				
	NO	NO	NO	AVG NO	SD NO
100	15.31858	16.11504	21.58407	15.71681	0.563182
10	5.938053	7.610619	-	7.011799	0.931953
1	16.50442	17.30973	17.16814	16.9941	0.42994
0.1	20.10619	19.70796	19.86726	19.89381	0.200438
0.01	21.78761	21.72566	21.64602	21.71976	0.070981
Concentration(µM)	Lycorine+Au@P				
	NO	NO	NO	AVG NO	SD NO
100	3.575221	3.707965	3.946903	3.743363	0.188352
10	0.823009	0.292035	0.548673	0.554572	0.265536
1	12.46018	11.61947	12.69027	12.25664	0.563669
0.1	18.40708	19.28319	19.00885	18.89971	0.448135
0.01	20.24779	19.87611	20.13274	20.08555	0.190283

[*] NO = Amount of nitrite

[**] AVG NO = Average of nitrite

[***] SD NO = Standard deviation of nitrite

VITA

Mr. Varayukrit Payuyong was born on July 20, 1988 in Nakhon Nayok, Thailand. He graduated from Nakhon Nayok Witthayakhom School in Nahhon Nayok with high school degree in 2006. He received his Bachelor's degree of Science, majoring in Biotechnology from King Mongkut's Institute of Technology Ladkrabang (KMITL, 2007-2010). And then, when he guaduated from KMITL, he joined Work and Travel program in Missouri, United States of America. After that, he has become a graduate student in the Biotechnology, Faculty of Science, Chulalongkorn University. Furthermore, he has joined the Biomaterial and Bioorganic Chemistry Research Research group under the direction of Associate Professor Dr. Nattaya Ngamrojanavanich. He graduated with Master's degree in Biotechnology of academic year 2016 from Chulalongkorn University.

Mr. Varayukrit Payuyong has attended the following conference for poster presentation.

International Conference on Research & Innovation In Food, Agriculture and Biological Sciences (RIFABS-16) scheduled on Dec. 12-13, 2016 at Phuket (Thailand).

Proceeding:

Payuyong, P., Ngamrojanavanich, N., and Muangsin, N. Combination of Gold Nanoparticles and Lycorine for Enhancing Anti-Inflammatory Activity. International Conference on Research & Innovation In Food, Agriculture and Biological Sciences (RIFABS-16), pp. 152-156. Phuket, Thailand, 2016.